63-4-6

(1)

THE PENNSYLVANIA STATE UNIVERSITY
Department of Engineering Mechanics

DEPT. of the ARMY PROJECT NO: DA-36-034-ORD-3576RD
ORD. MANAGEMENT STRUCTURE CODE NO: 5010.11.81500.01

Technical Report No. 2

SPHERICAL SHOCK WAVES IN SOLIDS

July 9, 1963

by

HARRY H. CALVIT and NORMAN DAVIDS

UNCLASSIFIED

UNCLASSIFIED

TECHNICAL REPORT NO. 2

July 9, 1963

SPHERICAL SHOCK WAVES IN SOLIDS

by

Harry H. Calvit and Norman Davids

~~DEPT. of the ARMY PROJECT NO.~~ DA-36-034-ORD-3576RD
ORD. MANAGEMENT STRUCTURE CODE NO: 5010.11.81500.01

THE PENNSYLVANIA STATE UNIVERSITY
Department of Engineering Mechanics

Technical Supervision by

BALLISTIC RESEARCH LABORATORIES
Aberdeen Proving Ground, Maryland

UNCLASSIFIED

TABLE OF CONTENTS

Acknowledgements

The work of this paper was sponsored by the Ballistic Research Laboratories, Aberdeen Proving Ground. Their support is gratefully acknowledged.

Acknowledgement is also due to O. T. Johnson of Ballistic Research Laboratories, for performing the experiments and A. Hoffman and R. E. Shear, also of Ballistic Research Laboratories, for many helpful suggestions.

LIST OF TABLES

LIST OF FIGURES

NOMENCLATURE

p	pressure
ρ	density
ρ_1	initial density
t	time
r,R	radius
u	radial particle velocity
c	sound speed
V	specific volume
V	volume
V_1	initial volume
γ	adiabatic exponent
A	constant
$\alpha,\beta,\delta,\epsilon$	self-similar exponents
U,D,P,π,V,R	self-similar functions
μ	$\sqrt{(\gamma-1)/(\gamma+1)}$
E, E_o	total energy
kb	kilobar
s	arc length, constant
S	entropy
C, $\dot{R}_s$	shock wave velocity
M	C/c Mach No.
T	temperature
Γ	Grüeneisen factor

ξ, λ, η	self-similar parameters
a	constant
$\bar{A}$	constant
PT	polytropic
QPT	quasi-polytropic
(U_o, P_o)	coordinates of S4
(U_1, P_1)	initial point or shock front
r_o	initial radius of cavity
t_o	"delay time"
ξ_1	value of ξ on shock front
R_s	shock radius
S	empirical factor
k	constant
cm	centimeter
x,v	translated coordinate system
A_1, A_2, A_3, A_4	constants
m	slope, mass
S1,S2,S3,S4	singular points
Cv	specific heat at constant volume
μ sec	microsecond
gm	gram
e	specific internal energy

CHAPTER I

INTRODUCTION

1.1 Reasons for Studying Spherical Shock Waves in Solids

The study of spherical shock waves in solids poses an interesting problem both from the standpoint of the desirability of the results as well as the inherent theoretical interest of the problem.

Information gained in this study should be of interest to investigators in many fields. The dynamic expansion of a spherical cavity in a metal under the conditions produced by a high explosive is closely related to several important problems. The phenomena associated with cratering due to hypervelocity impact, auto-frettage, underwater explosions, underground nuclear testing, nuclear reactor explosions, and many more have much in common with the cavity expansion problem.

The study of shock waves in solids and their applications to the study of properties of solids has become an active area of engineering and physics.

Propagation of these intense waves through solids with pressures up to 9 megabars has yielded fundamental thermodynamic data which could not be obtained by any other means. Shocks have been used to produce changes in crystal structure of some materials. It has also been found that shocks can change electrical insulators into conductors. Shocks harden metals, create and alter vacancies and dislocations in lattices and shock induced impact bonding of metals is now commercial.

It is felt that the simple geometry and relative ease of performing experiments warrants a rigorous study of spherical shock waves in solids.

1.2. Physics of Cavity Expansion Due to Explosive Impact

Consider a detonation initiated at the center of a spherical charge of high explosive surrounded by a ductile metal. A wave races through the explosive and imparts a sharp impact to the surrounding material. A shock wave is formed in the metal raising the the pressure to the order of magnitude of 500 kilobars. Under these extreme pressures the metal in a zone adjacent to the explosive behaves as a compressible, inviscid fluid. The shock wave propagates outward causing large plastic deformation, but decays due to spherical divergence, that is the pressure acts over an increasing area, into a stress wave.

Meanwhile in the gas there is a shock wave propagated back toward the center of symmetry which is reflected again causing the gas to pulsate until the pressure is sufficiently reduced.

Vibration or oscillation also takes place in the solid and for a finite body the problem of interaction from reflected waves arises.

Thus it becomes evident that the complications produced by the extreme pressures, the varying mechanical behavior of the metal, short time of the phenomena as well as the interaction between gas and solid pose a difficult problem in the study of shock waves in solids, if attempted in its full generality. An analytical theory can be formulated and carried through only by isolating the significant factors influencing the behavior of the metal. This will be done in later chapters of this work.

1.3. General Nature of Shock Waves

The concept of a shock wave is often misunderstood even among

scientific and engineering people. The label shock wave is often attached to both strong and weak discontinuities.

Weak discontinuities are fronts across which the time and/or space derivatives of the physical variables which describe the motion and state of the medium may experience a finite change. These will be referred to as "sound waves". These waves are the characteristics of the linear differential equations that describe the motion. Across a sound wave the physical variables experience only infinitesimal changes.

Strong discontinuities are fronts across which the physical variables which describe the motion and the state of a medium experience a finite change.

There are two types of discontinuity surfaces, contact surfaces and shock fronts. Contact surfaces are surfaces separating two parts of the medium without any flow across the surface. Shock fronts are discontinuity surfaces across which mass flows.

For these waves there exists no sonic transmission of the discontinuities of the physical variables since the governing differential equations are nonlinear. We find that the discontinuities of the physical variables cannot be described by a passage to a limit from continuous solutions as in the case of sound waves. To arrive at an adequate theory the physical fact of the existence of the shock wave must be taken into account.

It cannot be assumed that the motion is isentropic, since the velocity and temperature gradients are not small. Thus we are confronted with having to describe mathematically an irreversible thermo-

dynamic process. However, actual phenomena show that the irreversible zone is extremely narrow.

Outside of this transition zone the flow obeys the laws established for an adiabatic reversible process. Thus the empirical fact suggests a further mathematical idealization i.e., an infinitely thin transition zone. We find that the original differential equations, valid in the region of continuous flow, together with the conditions expressing the conservation laws and an entropy condition across the shock front, suffice to determine the flow without describing in detail the irreversible process across the shock zone.

There is considerable difference in the complexity of shock waves in gases and in solids. This explains the greater amount of literature on the former compared with the latter.

The difference in complexity of the two phenomena is attributable to several factors. One of the most significant being the lack of an equation of state for solids which is valid over a large range of pressures, and in general, a lack of knowledge of the thermodynamics of solids. (This is discussed in Section 4.9.) Another reason is the relative difficulty of making accurate measurements in solids. Other complications are (1) a shorter time sequence in solids, (2) material imperfections, (3) non-homogeneity, and lack of transparency as well as many others.

1.4. Statement of Problem and Scope of Study

The problem considered in this research is that of the dynamic behavior of a ductile thick spherical metal shell surrounding a

spherical charge of high explosive, subsequent to the detonation of the charge.

The problem is approached using a similarity theory (a one dimensional problem in which the motion can be described by one independent variable and hence the partial differential equations of motion are replaced by ordinary differential equations.) A more complete explanation of this type of theory is given in reference (4) page 146. Values for the velocity, pressure and density of the material are found for the early stages of the process. The results are compared with those of experiments. In addition, a critical study is made of the range of validity of similarity type solutions as they apply to shock waves in solids. A method of extending the self-similar theory is described.

Equations of state of solids are discussed and their compatibility with the theory of self-similar motion studied. A particular type equation of state called quasi-polytropic in this work is analyzed as to its compatibility with the similarity solution. Comparison is made between the shock relations obtained using this quasi-polytropic relation and the polytropic equation of state.

Experiments on thick aluminum spheres are described and the results are discussed.

CHAPTER II

BRIEF REVIEW OF PAST WORK

2.1. Elastic-Plastic Effects

The most significant work published on the problem of expansion of a spherical cavity in which elastic and elastic-plastic effects are emphasized was that by Hopkins (1)*. This article is a survey of the literature and includes comments on most of the significant work associated with the cavity expansion problem to date. Solutions are given for the elastic problem using the classical approach of integral transforms. It is of interest to mention that in the discussion of elastic-plastic waves, Hopkins emphasizes that due to the inhomogeneity of the displacement equation of equilibrium the plastic disturbances are not propagated at a definite velocity. Only that part of the plastic wave derivable from the plastic displacement potential travels at the plastic wave velocity.

It is also shown that even the relatively simple case of elastic-plastic effects in a perfectly plastic or Reuss type material that the location of the elastic-plastic boundary is not obtainable in closed form. An alternative procedure suggested by Hunter (2) is to specify the location of the interface and then determine the corresponding wave functions and applied pressure. The results obtained from this approach were in most cases found to be unrealistic or to place such severe limitations on the applied pressure as to be of little use.

---

*Figures in parenthesis appearing as superscripts refer to references listed in Bibliography.

Several interesting approximate solutions for large elastic-plastic deformation are also discussed as well as a numerical approach using the theory of characteristics.

2.2. Similarity Solutions of Equations of Gas Dynamics

Many articles have appeared in the literature on similarity solutions of the equations of gas dynamics. The particular equations which appear in this thesis were first presented by G. I. Taylor [3].

Taylor worked out a few numerical solutions as well as some approximate analytical solutions for an explosion in a perfect gas with γ ranging from 1.2 to 1.67. Subsequently or simultaneously analytic solutions appeared by Sedov [4], J. L. Taylor [5], Latter [6] and Sakurai [7]. Sedov presents the most complete discussion of the solution curve in the plane of the non-dimensional pressure and velocity functions. He discusses the singular points and their significance in the physical problem.

However, it is amazing that Courant and Friedrichs[8], who obviously were not aware that the exact solution existed, were able to deduce nearly as complete a description of the field of solution curves as Sedov.

2.3. Self-Similar Solutions of the Problem of Cratering Due to Hypervelocity Impact

As was mentioned earlier, the problem of blast waves in spheres and cratering due to hypervelocity impact have much in common. Consequently, the approach used in this thesis is similar to that used by several investigators of hypervelocity impact phenomena.

Davids and Huang [9] were apparently the first to approach the problem of cratering using the similarity or progressing wave theory. They applied the theory of self-similar flow using a perfect gas type equation of state for the target material and an energy criterion for establishing the crater depth. They assumed spherical symmetry in the problem.

Rae and Kirchner [10] formulated the problem more generally but succeeded in getting closed form solutions for the spherically symmetric case only. They also pointed out some restrictions on the equation of state and suggested ways of approaching the non-similar aspects of the problem. A material strength criterion was used to predict crater depth.

2.4. Numerical Solution of the Problems of Blast Waves In a Perfect Gas and Hydrodynamics of Hypervelocity Impact

Numerical solutions of the problem of strong blast waves in a perfect gas have appeared in the literature since about 1954. For the most part the approaches are all similar but there are some distinct differences.

Goldstine and Von Neumann [11] solve the problem of a strong point explosion in an ideal gas. The conservation laws of mass and momentum are combined and the resulting differential equation solved by finite differences. They employ an iterative scheme to satisfy the Rankine-Hugoniot conditions and use this as a check on the accuracy of their solution.

Brode [12] claims to be following the method of one of the previous

authors [13] and employs an artificial viscosity as a mechanism for avoiding shock-front discontinuities. The integration process consists of the step-wise solution of the difference equations which approximate the differential equations of motion of the gas.

Another somewhat different approach to the problem of a strong spherical blast wave in a gas is that used by P. D. Lax [14]. Lax uses the conservation form of the hydrodynamic equations and a slightly different way of differencing the equations.

One of the first investigators of the cratering problem using numerical techniques was Bjork. In predicting the crater due to meteroid impact, Bjork [15] assumed the impacted earth behaved as an inviscid, compressible fluid and postulated an equation of state for the material. In later investigations of hypervelocity impact in metals [16] this same model was assumed with favorable results.

Another investigator in the hypervelocity impact field is J. M. Walsh [17]. He has also developed a numerical program for the impact problem based on the "hydrodynamic" model.

CHAPTER III

SELF-SIMILAR SOLUTION OF PROBLEMS WITH SPHERICAL SYMMETRY

3.1. Theory

The theory of self-similar motion was originally conceived for the solutions of problems in gas dynamics. However, subsequent investigations have led to the admission of a broader class of problems.

(a) Basic Equations of Spherical Flow

The equations for spherical flow of a medium in Eulerean form expressing the conservation of momentum, mass and energy are

$$\frac{\partial u}{\partial t} + u \frac{\partial u}{\partial r} + \frac{1}{\rho} \frac{\partial p}{\partial r} = 0 \tag{3.1}$$

$$\frac{\partial \rho}{\partial t} + u \frac{\partial \rho}{\partial r} + \rho \left(\frac{\partial u}{\partial r} + \frac{2u}{r}\right) = 0 \tag{3.2}$$

$$\frac{De}{Dt} + p \frac{D}{Dt}\left(\frac{1}{\rho}\right) = 0 \tag{3.3}$$

where $\frac{D}{Dt} = \frac{\partial}{\partial t} + u \frac{\partial}{\partial r}$

and $e = f(p,\rho)$ is the form of the equation of state.

The Rankine-Hugoniot equations expressing conservation of mass, momentum and energy across the shock front are

$$\rho_1(u_1 - C) = \rho_2(u_2 - C) \tag{3.4}$$

$$\rho_1(u_1 - C)^2 + p_1 = \rho_2(u_2 - C)^2 + p_2 \tag{3.5}$$

$$e_2 - e_1 = \frac{1}{2}(p_1 + p_2)\left(\frac{1}{\rho_1} - \frac{1}{\rho_2}\right) \tag{3.6}$$

where subscripts 1, 2 refer to conditions in front of and behind the shock front respectively.

(b) Similarity Assumptions for a Strong Explosion

The approach used to determine the self-similar solution will be completely formal, and will employ a method commonly used in the solution of partial differential equations. That is, a particular solution of the partial differential equations is assumed reducing them to ordinary differential equations which are then solved. This treatment will be followed by a brief comment on dimensional considerations.

We seek a means by which we may obtain an analytic solution of the problem of a strong explosion in a continuous medium. In order to do so we introduce a variable $\xi = rt^{-\alpha}$ and the following assumptions:

$$\begin{aligned} u &= t^{\beta}\xi\, U(\xi) \\ p/\rho &= t^{\epsilon}\xi^2\, P(\xi) \\ \rho &= t^{\delta} D(\xi) \end{aligned} \tag{3.7}$$

where α, β, ϵ and δ are parameters, and U, D, P functions to be determined. By introducing these functions we shall show that the partial differential equationsof motion (Eqs. (3.1) - (3.3))are reduced to ordinary differential equations. The variable ξ defines geometrically a family of surfaces ξ = constant in the r,t-plane, one of which is the shock front. (This has been shown experimentally [18] to be a very

good assumption.

We now explore these solutions mathematically by substituting the expressions (3.7) into the equations of motion, giving respectively,

$$\xi t^{\beta-1}\,[\beta u - \alpha\,(\xi U'+U) + t^{\beta-\alpha+1}\,U(\xi U'+U) + t^{\epsilon-\alpha-\beta+1}\,(2P + \xi\,PD'/D + \xi P')] = 0 \tag{3.8}$$

$$t^{\delta-1}\,[(U-\alpha)\,\xi D' + \delta D + (\xi U' + 3U)D] = 0 \tag{3.9}$$

$$t^{\delta+\epsilon-1}\{-\gamma\xi^2\,P(\delta D-\alpha\xi D') + \xi^2\,[(\delta+\epsilon)\,DP - \alpha(2DP+\xi D'P + \xi DP')] + t^{\beta-\alpha+1}[-\gamma\xi^2 PD' + \xi(2DP + \xi D'P + \xi DP')]\,\xi U\} = 0 \tag{3.10}$$

where the equation of state $p = A\rho^{\gamma}$ has been used. This will be discussed in detail later in the thesis. These equations are now in a form where it is possible to eliminate the explicit factor t by properly choosing the exponents, thereby leaving a system of functions of one independent variable ξ. This is accomplished by letting

$$\epsilon = 2\beta \qquad \beta = \alpha-1 \tag{3.11}$$

so that $t^{\beta-\alpha+1} = t^{\epsilon-\alpha-\beta+1} = 1$.

Dividing by $\xi t^{\beta-1}$, $t^{\alpha-1}$, $t^{\delta+\epsilon-1}$ (which are not zero for $t > 0$) and simplifying the resulting equations, we obtain,

$$\beta U-\alpha(\xi U'+U) + U(\xi U'+U) + (2P + \xi PD'/D + \xi P') = 0 \qquad (3.12)$$

$$(U-\alpha)\ \xi D' + \delta D + (\xi U' +3U)D = 0 \qquad (3.13)$$

$$P'\xi(U-\alpha) + P[2\beta-\delta(\gamma-1) + 2(U-\alpha)]-(D'/D)P\xi(\gamma-1)$$
$$(U-\alpha) = 0 \qquad (3.14)$$

We now have a system of ordinary differential equations for the unknown functions $U(\xi)$, $D(\xi)$, $P(\xi)$ and two free parameters α and δ. The substitutions of Eqs. (3.7), which may appear artificial, are thus justified.

We shall now reduce the number of variables further. Solving Eq. (3.13) for $\xi D'/D$ gives

$$\xi D'/D = - (\delta+\xi U' + 3U)/(U-\alpha) \qquad (3.15)$$

When Eq. (3.15) is put into the remaining two equations we obtain the pair,

$$(U-\alpha)(\xi U'+U)+ \beta U + P[2\ (\delta+\xi U'+3U)/(U-\alpha)] + \xi P' = 0 \qquad (3.16)$$

$$-(\gamma-1)(\delta+\xi U'+3U) - 2\beta+(\gamma-1)\delta-2\ (U-\alpha)-(U-\alpha)\xi P'/P=0 \qquad (3.17)$$

These equations, linear in $\xi U'$ and $\xi P'$ may be solved simultaneously, giving

$$\xi U' = [-U(U-\alpha)(U-1) + (\delta+2\beta+3U\gamma)P]/\Delta \tag{3.18}$$

$$\xi P' = P\ (\gamma-1)U(U-1) - (U-\alpha)[(3\gamma-1)U-2] + \left(\left(\frac{2\beta-(\gamma-1)\delta}{U-\alpha}\right) + 2\gamma\right)P\ /\Delta \tag{3.19}$$

where $\Delta = (U-\alpha)^2 - \gamma P$.

By dividing Eq. (3.19) by Eq. (3.18), the following ordinary differential equation is obtained;

$$\frac{dP}{dU} = \frac{\xi P'}{\xi U'} = \frac{P[N(U) + PQ(U)]}{R(U) + P(S(U))} \quad . \tag{3.20}$$

After the simplification,

$$\begin{aligned} N(U) &= \gamma U(3\alpha-1-2U) + (3-\alpha)U-2\alpha \\ Q(U) &= [2\beta -(\gamma-1)\delta] /(U-\alpha) +2\gamma \\ R(U) &= U(U-\alpha)(1-U) \\ S(U) &= \delta+2\beta+ 3U\gamma \end{aligned} \tag{3.21}$$

This is the basic differential equation for self-similar motion. After the appropriate solution has been found for $P = P(U)$, the function $\xi = (U)$ is found by a quadrature of Eq. (3.18) and the density function $D(\xi)$ is obtained from Eq. (3.15).

As we shall see, these self-similar solutions provide a sufficiently general mathematical description of an expanding cavity reasonably consistent with the given conditions of iniation of the process.

There remains the problem of choosing the two parameters α and δ.

Let us assume that the total energy given up by the explosive appears as kinetic and potential energy in the surrounding medium. This is a reasonable one for the cavity expansion process, because of its short duration, provided certain secondary effects are neglected. With $\xi = \xi_1$ representing the shock front at a time t, the total energy in the fluid shell (potential + kinetic) at time t is given by

$$E(t) = \int_{r_o}^{r_1} \left(\frac{p}{\gamma-1}\right) 4\pi r^2 dr + \int_{r_o}^{r_1} \frac{1}{2} \rho u^2 4\pi r^2 dr \qquad (3.22)$$

where $r_o = \xi_o t^\alpha$ is an arbitrary member of the family and $r_1 = \xi_1 t^\alpha$ is the location of the shock front.

The first term arises from the polytropic relation $p=A\rho^\gamma$ which has been assumed for the material and the fact that the work done by the material in becoming compressed from an initial volume V_1 to a a volume V is given by

$$E(V) = \int_{V_1}^{V} pdV = \rho_1 V_1 \int_{\rho_1}^{\rho} A\rho^\gamma \left(-\frac{d\rho}{\rho^2}\right) = -\frac{pV}{\gamma-1} + \text{const.} \qquad (3.23)$$

where we have used the relation $\rho_2 V_2 = \rho_1 V_1$. Using the substitutions in (3.7) the energy expression becomes

$$E(t) = 4\pi \int_{r_o}^{r_1} (t^{\delta+\epsilon} \frac{P}{\gamma-1} + \frac{1}{2} t^{\delta+2\beta} U^2)\xi^2 D(\xi) r^2 dr$$

Substituting $r=\xi t^{\alpha}$, $dr=t^{\alpha}d\xi$ into the preceding equation and noting that t is constant,

$$E(t) = 4\pi\, t^{\delta+5\alpha-2} \int_{\xi_o}^{\xi_1} (\frac{P}{\gamma-1} + \frac{1}{2} U^2)\xi^4 D(\xi) d\xi \quad . \tag{3.24}$$

Since the integral is independent of t, we make the energy independent of time by satisfying the relation

$$\delta+5\alpha-2 = 0 \qquad \text{or} \qquad \delta=2-5\alpha \tag{3.25}$$

We shall narrow down the number of parameters by examining the compatibility of our solution with the basic Rankine-Hugoniot conditions across a shock front. If the undisturbed and disturbed medium parameters are u_1, ρ_1, p_1 and u_2, ρ_2, p_2, respectively and the shock wave velocity is C, then the relations for (see (8) p.123-4), conservation of mass, momentum and energy across the shock front are,

$$\rho_1(u_1-C) = \rho_2(u_2-C) = m \tag{3.26}$$

$$\rho_2 u_2(u_2-C) - \rho_1 u_1(u_1-C) = p_1-p_2 \tag{3.27}$$

$$\rho_2(\tfrac{1}{2}u_2^2+C)(u_2-C)-\rho_1(\tfrac{1}{2}u_1^2+C)(u_1-C) = p_1u_1-p_2u_2 \tag{3.28}$$

where $e = \frac{1}{\gamma-1} p/\rho$ for a polytropic medium.

When the undisturbed state is a medium at rest, with $u_1=0$, these equations reduce to

$$\rho_2(C-u_2) - \rho_1 C = 0 \tag{3.29}$$

$$\rho_2 u_2(C-u_2) - (p_2-p_1) = 0 \tag{3.30}$$

$$\rho_2\left(\frac{1}{2}u_2^2 + \frac{1}{\gamma-1}\frac{p_2}{\rho_2}\right)(C-u_2) - p_2u_2=0 \quad (e_1=0) \tag{3.31}$$

It is useful to solve Eq. (3.29) and (3.30) for the velocities. Then

$$u_2 = (p_2-p_1)/\rho_1 C \tag{3.32}$$

$$C = \sqrt{\frac{\rho_2}{\rho_1}\left(\frac{p_2 - p_1}{\rho_2 - \rho_1}\right)} \tag{3.33}$$

If p is in kilobars, ρ in gm/cc, then u and C will come out in km/sec as expressed by the following formulas:

$$u_2 = (p_2 - p_1)/(10\ \rho_1 C)$$
$$C = \sqrt{\frac{\rho_2}{\rho_1}\ \frac{p_2 - p_1}{10(\rho_2-\rho_1)}} \tag{3.34}$$

It is useful to have these relations for a polytropic medium. Then

$$u_2 = \sqrt{\frac{2}{\gamma-1}\ \frac{p_2}{\rho_2}\ \frac{p_2 - p_1}{(p_2 + p_1)}}$$
$$C = \frac{1}{1 - \frac{\rho_1}{\rho_2}}\ \sqrt{\frac{2}{\gamma-1}\ \frac{p_2}{\rho_2}\ \frac{p_2 - p_1}{p_2 + p_1}} \tag{3.35}$$

From (3.32), with $\mu = \sqrt{(\gamma-1)/(\gamma+1)}$, and if p_1 is negligible,

$$u_2 = C(1 - \mu^2)$$

$$p_2 = \rho_1 u_2 C = \rho_1 C^2 (1 - \mu^2) \qquad (3.36)$$

$$\rho_2/\rho_1 = (\gamma+1)/(\gamma-1) = \frac{1}{\mu^2}$$

$$c = \sqrt{\frac{dp}{\partial\rho}} = \sqrt{1 + \mu^2}\ C$$

The last quantity is conveniently referred to as the "sound speed" in shock wave analysis. These relations apply just as well to a spherical or curved surface as to a plane, since the effect of spherical divergence (the $2u/r$ term) on a finite or sudden jump is of a higher order of magnitude. This may also be shown geometrically by considering an infinitesimal surface element of the shock front. Since $\xi_1 = rt^{-\alpha}$ (by definition) along the shock front,

$$0 = t^{-\alpha}\, dr - \alpha r t^{-\alpha-1}\, dt$$

so $C = \frac{dr}{dt} = \alpha r t^{-1} = \alpha \xi_1 t^{\alpha-1}$. Then from Eq. (4.7) and the relations (3.29) through (3.31) with

$$C - u_2 = \alpha \xi_1 t^{\alpha-1} - t^{\beta} \xi_1 U(\xi_1) = \xi_1 t^{\beta}(\alpha - U),$$

we obtain

$$t^{\delta+\beta}\, \xi_1\, D(\alpha-U) - \rho_1\, \alpha\, \xi_1\, t^{\beta} = 0 \qquad (3.37)$$

$$t^{\delta+2\beta}\, \xi_1^2\, DU\, (\alpha-U) - t^{\delta+2\beta}\, \xi_1^2\, DP = 0 \qquad (3.38)$$

$$t^{\delta+3\beta} D\xi_1^2 \left(\frac{1}{2} U^2 + \frac{1}{\gamma-1} P\right) \xi_1 (\alpha-U) - t^{\delta+3\beta} \xi_1^3 DPU = 0 \quad (3.39)$$

We note that the time factor cancels in Eq. (3.38) and Eq. (3.39), so that these equations are automatically satisfied. However, to secure independence of time in Eq. (3.37), it is necessary to make

$$\delta = 0 \quad . \quad (3.40)$$

With this condition and the relations (3.25), the assumed form for the progressing wave solutions reduce to

$$u = (r/t)\, U(\xi) \qquad P = (r/t)^2\, D(\xi) P(\xi)$$

$$\rho = D(\xi) \qquad p/\rho = (r/t)^2\, P(\xi) \quad (3.41)$$

$$\text{with} \quad \xi = rt^{-\alpha}$$

This solution shows that on the shock front, where ξ is constant, the physical quantities such as velocity, pressure, density, and wave velocity are constant on the rays r/t = constant. This also dimensionalizes the functions (4.7) correctly, for, with ξ having the dimensions of length per $(\text{time})^{\alpha}$, and

$$\xi = [LT^{-\alpha}] \qquad D(\xi) = [ML^{-3}]$$

$$U(\xi) = [1] \qquad P(\xi) = [1]$$

then u, p, ρ, p/ρ have respectively the correct dimension of velocity, pressure $(ML^{-1}T^{-2})$, density and velocity squared. The com-

plete set of exponents is now

$$\alpha = 2/5 \qquad \epsilon = -6/5$$
$$\beta = -3/5 \qquad \delta = 0 \quad . \tag{3.42}$$

If we now turn to purely dimensional considerations the following are recognized as the system of fundamental parameters influencing the motion of the medium: ρ_1, p_1, E_o, r, t, γ. From these we can form only three independent dimensionless quantities: γ ; $\lambda = \frac{\rho_1^{1/5} r}{E_o^{1/5} t^{2/5}}$; $\tau = \frac{p_1^{5/6} t}{E_o^{1/3} \rho_1^{1/2}}$. For a strong shock $(p_1 << p_2)$ the system reduces to only γ ; $\lambda E_o^{1/5}/\rho^{1/5} = rt^{-2/5}$. If we take γ to be constant, we see that the motion can be described by only one independent variable, λ , which agrees with our earlier findings.

We can then write (see Sedov, Ref. (4))

$$u = (r/t)\, V(\lambda) \quad , \quad p = \frac{a}{r^{k+1}}\, t^{s+2}\, \pi(\lambda)$$
$$\rho = \frac{a}{r^{k+3}}\, t^{s}\, R(\lambda) \qquad a = [ML^kT^s] \tag{3.43}$$

This system of equations differs from the ones previously derived only in the dimensional sense. Here π, V and R are all dimensionless functions of λ and are related to the functions P, U, D in the following way: $U = V$, $R = D/\rho_1$, $P = \pi\rho_1/D = \frac{\pi}{R}$.

Another means of approaching the problem is to consider a flow field which depends on a non-dimensional parameter $\eta = r/R_s(t)$. At each instant the distributions of velocity, pressure and density are taken to be the same when viewed on a scale defined by the shock radius at that instant. Then if we assume the radius of the shock wave follows a law $R_s(t) = \bar{A}\, t^n$, we find we have essentially the same formulation as discussed earlier. All that remains is the introduction of the dimensionless velocity, pressure and density functions which are functions of η.

3.2. Solution of the Governing Differential Equation of Self-Similar Motion

The analytical solution of the governing ordinary differential equation is obtained in an indirect way (see Sedov (Ref. 4)). We recall that in the first section of this chapter we used the fact that the energy integral was time independent to obtain a relationship between the parameters α and δ.

It can be shown that the energy assumption implies

$$\xi^5[PU + (U-\alpha)\,(\frac{\gamma U^2}{2} + \frac{P}{\gamma-1})]D = \text{constant}. \qquad (3.44)$$

This must be true for all stages of the process, in particular on the shock front. Evaluation of the constant from the Rankine-Hugoniot conditions shows it to be zero. Hence, we have effectively obtained an integral of Eq. (3.20) and the relationship between P and U becomes

$$P = (\gamma-1)\, U^2\, (U-\alpha)/2\,(\alpha-\gamma U) \qquad (3.45)$$

Relations can then be determined for $D = D(\xi)$, $U = U(\xi)$, $P = P(\xi)$ using equations (3.15), (3.18) and (3.19).

A discussion of the singular points of the differential equation (3.20) and the solution curve (3.45) are given in Chapter IV.

CHAPTER IV

APPLICATION OF THE THEORY OF SELF-SIMILAR MOTION TO THE PROBLEM OF EXPANSION OF A SPHERICAL CAVITY IN A METAL DUE TO EXPLOSIVE IMPACT

4.1. Description of Model and Assumptions

Detonation of a high explosive confined within and in contact with a ductile metal generates a strong shock wave which raises the pressures abruptly (i.e., in negligible time) into the megabar range. These pressures are large compared to the material strength even at high strain rates and one is led to assume that the medium behaves as an inviscid, compressible fluid.

Thus the solution of the problem of spherical blast waves in a metal originating at a spherical cavity reduces to solving the equations of fluid mechanics (3.1) - (3.4) (i.e., conservation of mass, momentum and energy, together with the equation of state of the medium).

If we next assume that the motion is self-similar, then all of the ideas discussed in Chapter III are at our disposal. The remaining question is that of the equation of state. In this work it has been assumed to be of the form $p = A\rho^{\gamma}$. This is justified to some extent in the next section.

4.2. Equations of State of Metals

The equation of state plays a central part in the application of the theory of self-similar motion to shock waves in metals. In addition to furnishing a relationship between pressure and density, it furnishes a criterion for the termination of the regime in which the

self-similar assumptions are valid.

The notion of an equation of state of a medium implies thermodynamic equilibrium and can be described by a functional relationship between any three of the variables p, V, T, S, e. Thus there exists several forms of the equation of state of a pure substance.

Consider the Helmholtz work function

$$F = e - TS$$

From this and the first and second laws of thermodynamics follows

$$dF = de - TdS - SdT = - pdV - SdT$$

Now dF is an exact differential of the thermodynamic potential function and hence

$$\frac{\partial^2 F}{\partial V \partial T} = \left(\frac{\partial S}{\partial V}\right)_T = \left(\frac{\partial p}{\partial T}\right)_V$$

Since

$$\left(\frac{\partial e}{\partial V}\right)_T = T\left(\frac{\partial S}{\partial V}\right)_T - p = T\left(\frac{\partial p}{\partial T}\right)_V - p$$

it follows that

$$de = \left(\frac{\partial e}{\partial T}\right)_V dT + \left(\frac{\partial e}{\partial V}\right)_T dV$$

$$= C_V dT + \left[T\left(\frac{\partial p}{\partial V}\right)_T - p\right]dV$$

An ideal gas is defined as a medium which possesses no intermolecular forces of restraint; this implies that the internal energy is a function of temperature alone, hence $(\frac{\partial e}{\partial V})_T = 0$ and

$$T(\frac{\partial p}{\partial T})_V - p = 0$$

or

$$p = Tg(V) = Tf(\rho) \tag{4.1}$$

Now a solid possesses energy due to the presence of intermolecular forces and a thermal energy associated with molecular vibrations. Hence even at absolute zero the energy of a solid is non-zero. Thus, we can express the energy of a solid mathematically as

$$e = f(V) + Tg(V) \tag{4.2}$$

Another formulation for the higher pressure range called the Mie-Grüneisen [10] equation is

$$e(p,\rho) - e_c(\rho) = \frac{p - p_c(\rho)}{\rho \Gamma(\rho)} \tag{4.3}$$

The subscript c refers to the cohesive contribution and Γ is the Grüneisen constant which depends weakly on ρ.

By rewriting equation (4.3) in another form the measured shock wave data along the Hugoniot curve can be used to calculate the cohesive contribution.

$$e_H(\rho) - e_c(\rho) = \frac{p_H(\rho) - p_c(\rho)}{\rho \Gamma(\rho)} \tag{4.4}$$

Subtracting (4.4) from (4.3) we obtain

$$e - e_H(\rho) = \frac{p - p_H(\rho)}{\rho \Gamma(\rho)}$$

The Mie-Grüneisen equation can be rewritten in the form

$$e = \frac{p}{\rho \Gamma(\rho)} - \Delta(\rho)$$

and we find

$$\Delta(\rho) = \frac{p_c(\rho)}{\rho \Gamma(\rho)} - e_c(\rho) = \frac{p_H(\rho)}{\rho \Gamma(\rho)} - e_H(\rho) \qquad (4.5)$$

The last expression can be found from shock wave data and in this way the magnitude of $\Delta(\rho)$ can be determined.

It has been found [4] that the only form of the equation of state compatible with the self-similar flow assumption is of the form

$$e = p\varphi(\rho) \quad .$$

We see that the leading term of the Mie-Grüneisen equation is $p/\rho\Gamma(\rho) = p\varphi(\rho)$ and we are forced to use only this part of the equation in the self-similar solution. Thus the assumption is accurate so long as the term $\Delta(\rho)$ is small compared to $p/\Gamma(\rho)$. It should be pointed out that it does not follow that the fluid assumption is invalid when $\Delta(\rho)$ is not small compared to $p/\rho\Gamma(\rho)$.

The Grüneisen factor Γ has been assumed to be a constant equal to $(\gamma-1)$. This is not absolutely necessary since the variation of Γ

could be taken into account but has been dropped for convenience.

For fixed parameters α, β, ϵ, δ the solution $P = P(U)$ of the governing differential equation (3.20) is seen to depend on γ. The value of γ determines the location of the singular points and other significant aspects to be discussed in more detail in the next section.

In determining the single value of γ to be used, we must realize that the γ which best describes the state for one point in the medium will certainly be a poorer approximation for another point.

If a straight line is fitted the shock wave data from Ref. (19) and is considered as representing only the high pressure range, an equation of state for the metals considered is obtained. These are actually Hugoniot curves, but will be used to approximate the isentropes of the metals (See Huang [20]).

We will now consider a particular equation of state $p=A((\rho/\rho_1)^{\gamma}-1) = A\rho^{\gamma} - B$ called quasi-polytropic in this thesis . This equation is very similar to the polytropic equation of state and is used by many authors to describe the equation of state for dense media, since $p = 0$ does not imply $\rho = 0$ as for gases. Comparison is made between the polytropic and quasi-polytropic equations with respect to relations predicted by each equation or shock front relations, sound speed, and thermodynamic relations. The inability of the quasi-polytropic equation to be used in a self-similar theory is also exhibited.

The sound speed for a PT gas $p = A\rho^{\gamma}$ is

$$c^2 = dp/d\rho = \gamma A\rho^{\gamma-1}$$

for a QPT

$$c^2 = \frac{d}{d\rho}(A\rho^\gamma - B) = \gamma A\rho^{\gamma-1}$$

For later use we will define

$$\bar{p} = p + B = A\rho^\gamma.$$

Consider next specific internal energy. For a PT medium;

$$e = \frac{pV}{\gamma-1}$$

For a QPT medium;

$$e = \int -(A\rho^\gamma - B)\, d(\tfrac{1}{\rho})$$

$$= \left(\frac{A}{\gamma-1}\rho^{\gamma-1} - \frac{B\rho^{-1}}{-1} \right)$$

$$= \left(\frac{\bar{p}}{\gamma-1} + B \right)V$$

$$e = \left(\frac{p + \gamma B}{\gamma-1}\right)V \tag{4.6}$$

The Hugoniot function is defined by

$$H(V,p) = e(V,p) - e(V_1,p_1) + (V-V_1)\left(\frac{p + P_1}{2}\right) \tag{4.7}$$

If we set $H(V,p) = 0$, the Hugoniot relation is obtained. This relation characterizes all pairs (V,p) for the state on one side of the shock front that are compatible with the three shock front conditions

when the values (V_1,p_1) on the other side are prescribed. For a polytropic equation of state it is a rectangular hyperbola (Fig. 1).

For a QPT medium

$$H(V,p) = \frac{1-\mu^2}{2\mu^2}(p+\gamma B)V - \frac{1-\mu^2}{2\mu^2}(p_1 + \gamma B)V_1 + (V-V_1)\left(\frac{p_1 + p}{2}\right)$$

$$2\mu^2 H = (1-\mu^2)(pV) + (1-\mu^2)\gamma BV - (1-\mu^2)p_1V_1 - (1-\mu^2)\gamma BV_1 + 2\mu^2(V-V_1)\left(\frac{p + p_1}{2}\right)$$

$$2\mu^2 H = (V-\mu^2V_1)p - (V_1-\mu^2V)\,p_1 + (1-\mu^2)\,\gamma B(V-V_1) \qquad (4.8)$$

Figure (1) shows the Hugoniot for PT and a QPT medium plotted for the purpose of comparison (p_1 has been assumed equal to zero).

For the case of a shock moving into a gas at rest we obtain

$$(V-\mu^2V_1)[p + (1-\mu^2)\gamma B] = V_1\,(1-\mu^2)B.$$

This can be rewritten as

$$p_2 = -\frac{(1-\mu^2)\gamma B}{V_2 - \mu^2V_1}\,(V_2-V_1)$$

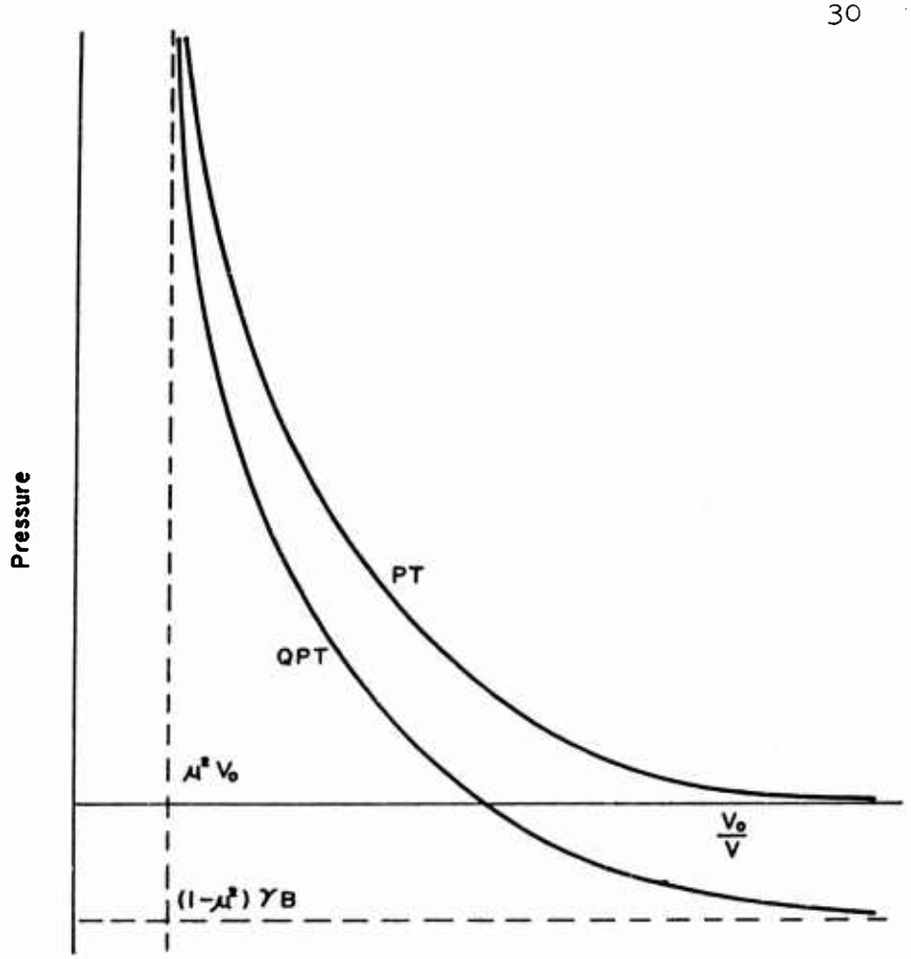

FIG. 1 - HUGONIOTS FOR A POLYTROPIC AND QUASI-POLYTROPIC MEDIUM

also

$$\frac{\rho_2}{\rho_1} = \frac{p_2 + \frac{2\gamma}{\gamma+1} B}{\mu^2 p_2 + \frac{2\gamma}{\gamma+1}} = \frac{\bar{p}_2 + \mu^2 \bar{p}_1}{\bar{p}_1 + \mu^2 \bar{p}_2} \tag{4.9}$$

Thus we see that for a QPT medium the ratio $\frac{\rho_2}{\rho_1}$ is not a constant as in the case of a PT medium; since $\bar{p}_1 \neq 0$. Next consider using the QPT relation for self-similar motion. In order to obtain the solution curve of the differential equation we must have a unique starting point in the P-U plane. Since the ratio $\frac{\rho_2}{\rho_1}$ is not constant there exists no such point and we are forced to abandon the QPT relation.

4.3. Solution of the Blast Wave Problem in Aluminum

For a shock wave moving into polytropic medium at rest, the Rankine-Hugoniot equations become

$$\rho_2 (C - u_2) - \rho_1 C = 0 \tag{4.10}$$

$$\rho_2 u_2 (C - u_2) - (p_2 - p_1) = 0 \tag{4.11}$$

$$\rho_2 (\tfrac{1}{2} u_2^2 + \frac{1}{\gamma-1} \frac{p_2}{\rho_2})(C - u_2) - p_2 u_2 = 0 \tag{4.12}$$

$$(e_1 = 0)$$

It is interesting to estimate the accuracy of the assumption of a strong shock wave.

To do so the above equations are rewritten in another form using (3.32) through (3.36). That is,

$$u_2 = \frac{2}{\gamma+1} C \left[1 - \left(\frac{c}{C}\right)^2\right] = \frac{2C}{\gamma+1} f_1$$

$$\rho_2 = \frac{\gamma+1}{\gamma-1} \rho_1 \left[1 + \frac{2}{\gamma-1} \left(\frac{c}{C}\right)^2\right] = \frac{\gamma+1}{\gamma-1} \rho_1 f_2 \qquad (4.13)$$

$$p_2 = \frac{2}{\gamma+1} \rho_1 C^2 \left[1 - \frac{\gamma-1}{2\gamma} \left(\frac{c}{C}\right)^2\right] = \frac{2}{\gamma+1} \rho_1 C^2 f_3,$$

Figure (2) shows the values of f_1, f_2, f_3 plotted against $\frac{c}{C} = \frac{1}{M}$.

If we assume $p_1 = 0$ which is equivalent to setting $f_1 = f_2 = f_3 = 1$ and $\frac{c}{C} = 0$, then the expressions for u_2, ρ_2, p_2 become:

$$u_2 = \frac{2}{\gamma+1} C \qquad (4.14)$$

$$\rho_2 = \frac{\gamma+1}{\gamma-1} \rho \qquad (4.15)$$

$$p_2 = \frac{2}{\gamma+1} \rho_1 C^2 \qquad (4.16)$$

Now $\xi = \xi_1$, on the shock front and we can write

$$\left(\frac{R_s}{t}\right) U(\xi_1) = \frac{2}{\gamma+1} \frac{d}{dt} \left(\xi_1 t^{\alpha}\right)$$

$$\frac{R_s}{t} U(\xi_1) = \alpha \left(\frac{2}{\gamma+1}\right) \xi_1 t^{\alpha-1}$$

$$\frac{R_s}{t} U(\xi_1) + \alpha \left(\frac{2}{\gamma+1}\right) R_s t^{-\alpha} t^{\alpha-1}$$

$$U(\xi_1) = \frac{2\alpha}{\gamma+1} \qquad (4.17)$$

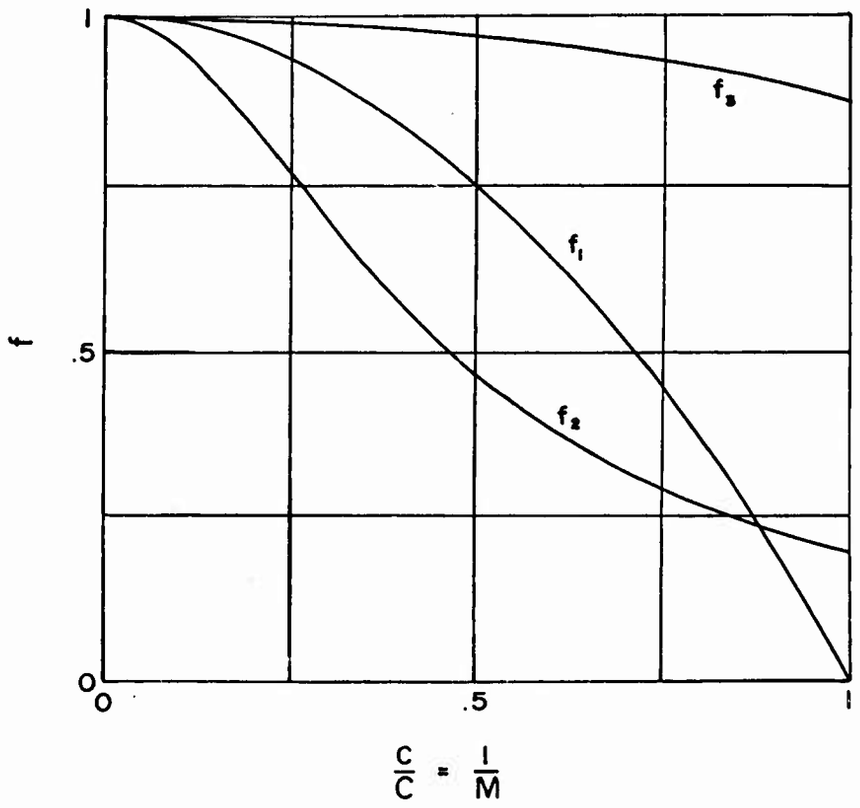

FIG. 2 – VARIATION OF THE FUNCTION f_1, f_2, f_3 WITH $\frac{C}{C}$

Following the same procedure for $P(\xi_1)$ and $D(\xi_1)$ we find

$$P(\xi_1) = 2\,\alpha^2\,\mu^2 / (\gamma+1)$$
$$D(\xi_1) = \rho_1 / \mu^2 \qquad (4.18)$$

For aluminum with $\gamma = 7.6$ this supplies an initial point in the P-U plane. The solution curve is the unique integral of (3.20) which passes through this point and the singular point D, as shown in Fig. 3.

We need next to prescribe the initial conditions at the boundary of the cavity and the total energy supplied by the explosive. We will see how these allow us to determine ξ_1, and consequently, the motion of the shock front.

From private communication with R. E. Shear of Ballistic Research Laboratories, Aberdeen Proving Grounds, we found that for pentolite under confinement the detonation pressure would be around 400 kb. For convenience, a value of pressure = 384 kb was used in this work. This pressure predicts the proper density ratio using the Hugoniot equation (Fig. 4) as the equation of state for the material at the cavity surface.

The next step is to assure that when the shock wave is at the cavity surface, the pressure and density have the right values, namely

$$p = \left(\frac{r_o}{t_o}\right)^2 P(\xi_1)\, D(\xi_1) \qquad (4.19)$$

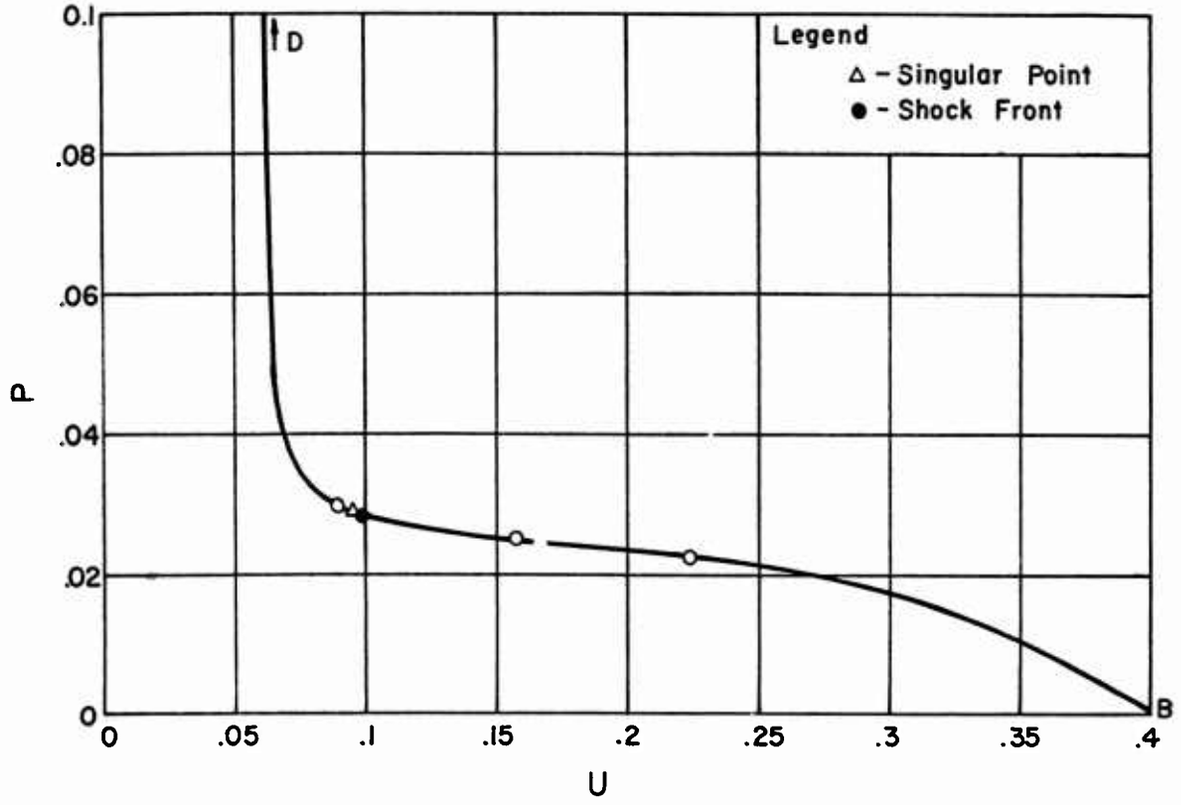

FIG. 3 – SOLUTION CURVE FOR ALUMINUM $\gamma = 7.6$

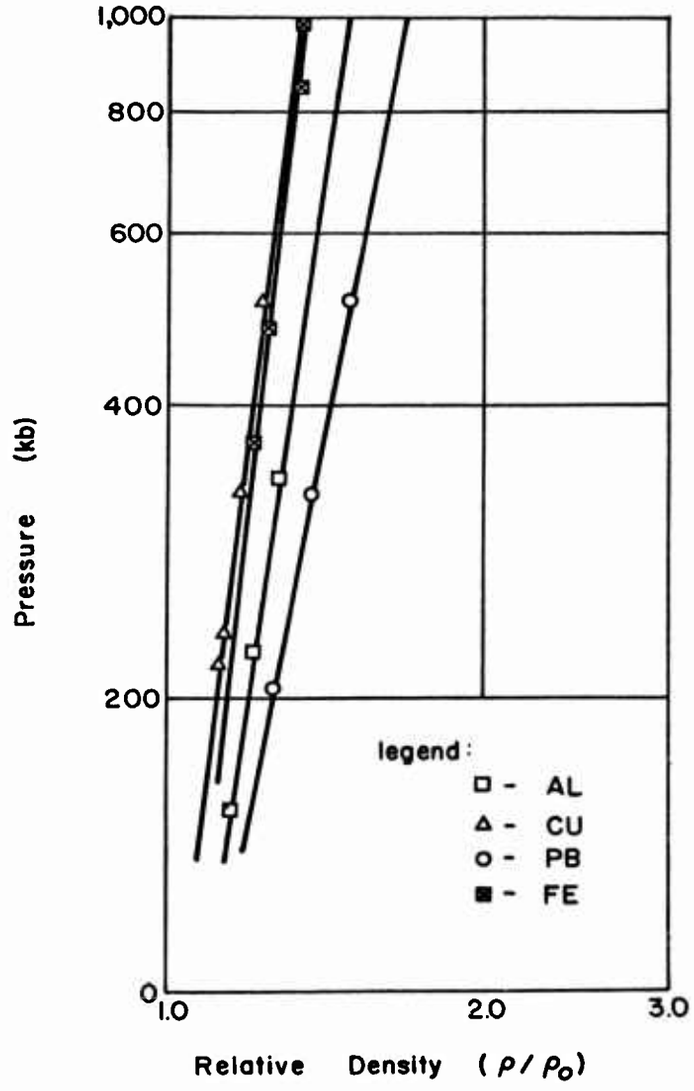

FIG 4 — HUGONIOTS OF FOUR METALS

In this expression p, ρ, r_o, P and D are known, and t_o is determined, i.e.,

$$t_o = r_o \left(\rho/p\ P(\xi_1)\ D(\xi_1)\right)^{1/2}$$

The values used to calculate t_o were

$$\rho_1 = 2.785 \text{ g/cc}$$

$$p = 384 \text{ kb}$$

$$r_o = 1.698 \text{ cm}$$

$$P(\xi_1) = 0.0286$$

$$D(\xi_1) = 3.5182 \text{ g/cc}$$

as indicated in Fig. 11 and Table 2. Using these values we find $t_o = 0.868\ \mu$ sec.

This value of t is the "delay" time to assure the proper position of the shock front at the initiation of the expansion process.

With the values of r_o, t_o known, ξ_1 is calculated from the definitive relation $\xi = rt^{-\alpha}$. Then

$$\xi_1 = r_o\ t_o^{-\alpha} = 451.28 \text{ cm/sec}^{2/5}.$$

The velocity of the shock wave is given explicitly by the expression

$$C = \frac{dR_s}{dt} = \frac{d}{dt}\ (\xi_1\ t^{\alpha})$$

or

$$C = 2/5\ (451.28)\ t^{-3/5} \text{cm/sec}$$

$$= 181\ t^{-3/5}\ \text{cm/sec}\ . \qquad (4.20)$$

The physical variables immediately behind the shock wave are given by equations (4.14) through (4.16). That is

$$u_2 = \frac{2}{\gamma+1}\ C = \frac{2}{7.6+1}\ (181)t^{-3/5}$$

$$= 42.0\ t^{-3/5}\ \text{cm/sec} \qquad (4.21)$$

$$\rho_2 = \frac{8.6}{6.6}\ \rho_1 = 3.518\ \text{g/cc} \qquad (4.22)$$

and

$$p_2 = \frac{2}{8.6}\ (2.785)\ (181\ t^{-3/5})^2$$

$$= 2.13 \times 10^{-5}\ t^{-6/5}\ \text{kb} \qquad (4.23)$$

In order to describe the distribution of the variables through the medium between the shock wave and cavity surface, we turn to the solution of the differential equation (3.20). The solution of the blast wave problem was exhibited as $P = P(U)$. It was shown that the functions $P = P(\xi)$, $U = U(\xi)$, $D = D(\xi)$ could be obtained by quadrature of Eqs. (3.15), (3.18) and (3.19). However, it was found to be more convenient to proceed in a different manner.

A numerical integration of the differential equation (3.20) was performed. (See Appendix B). At the same time, particle "paths" were traced out and the variation of the physical variables along these particle paths were calculated. (See Appendix B).

Pressure isobars were then drawn connecting the points of equal pressure in the medium. (See Fig. 5).

Particular attention was paid the particle which started at $r = r_o = 1.698$ as this marked the cavity surface and was of great interest in the study. (Figs. 5,6,8,9). It is also convenient to tabulate the energy integral (3.24) and compare it at some selected time to the energy given up by the explosive.

In the theory of self-similar motion, an assumption of constant energy was made (See Eq. (3.24)) in order to provide the condition (3.25) for determining α and with it, all the other exponents. The energy integral (3.24) is extended between two points, one of which is located on the shock front $\xi = \xi_1$ and a lower value $\xi = \xi_o$. The integral path, such as BC in Fig. 6 may be arbitrarily chosen, so long as it terminates on these two curves.

The energy in the disturbed part of the solid will, however, change with time because its lower boundary, the cavity surface, is not one of the family of ξ-curves. Thus, the energy values in Table (1) represent an integration of the expression in (3.25) taken along the cavity surface curve. If we extend this integration far enough (say to 100 microsec) so that point D practically coincides with point C, the values in the table become asymptotically constant, and we have

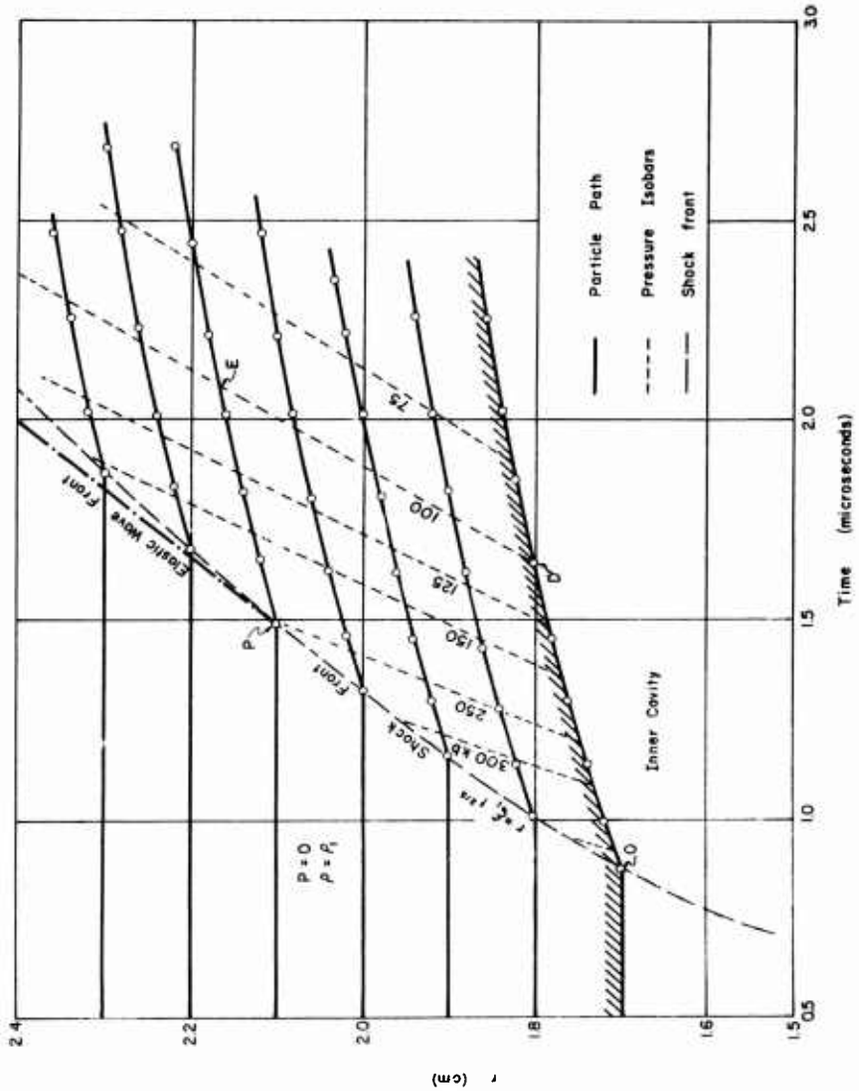

FIG. 5 — r, t - DIAGRAM OF SHOCK REGION FOR ALUMINUM SPHERE

$$E = \int_A^C = \int_A^B + \int_B^C = 0 + \int_B^D = - \int_{\xi_o}^{\xi_1}$$

From Table 1 we see that the energy does tend to be a constant and we have just shown that this limit is the value of the energy integral (3.25).

If we now suppose that all (or any known fractional part) of the energy given up by the explosive is transmitted into the solid, then the shock process could be terminated when the energy reaches the amount available. It is not possible to determine a precise point of time because of the asymptotic way in which the energy increases. It is seen, however, that E reaches 90% of its ultimate value in 3 micro-seconds, which is a very short time compared with the expansion process.

The post-shock expansion presumably must take place under constant energy conditions for a "long" period of time, until it is dissipated by viscosity of the flow, elastic waves and other side effects.

For energy available in the explosive, Shear [21] gives the value

$$E_{Total} = 1.152 \quad k \text{ cal/g}$$

which, for our explosive weight of 0.07 lb, gives

$$E_{Total} = 1.26 \times 10^{12} \text{ ergs.}$$

Our calculated asymptotic value (Table 1) from the energy integral comes to 96% of this value.

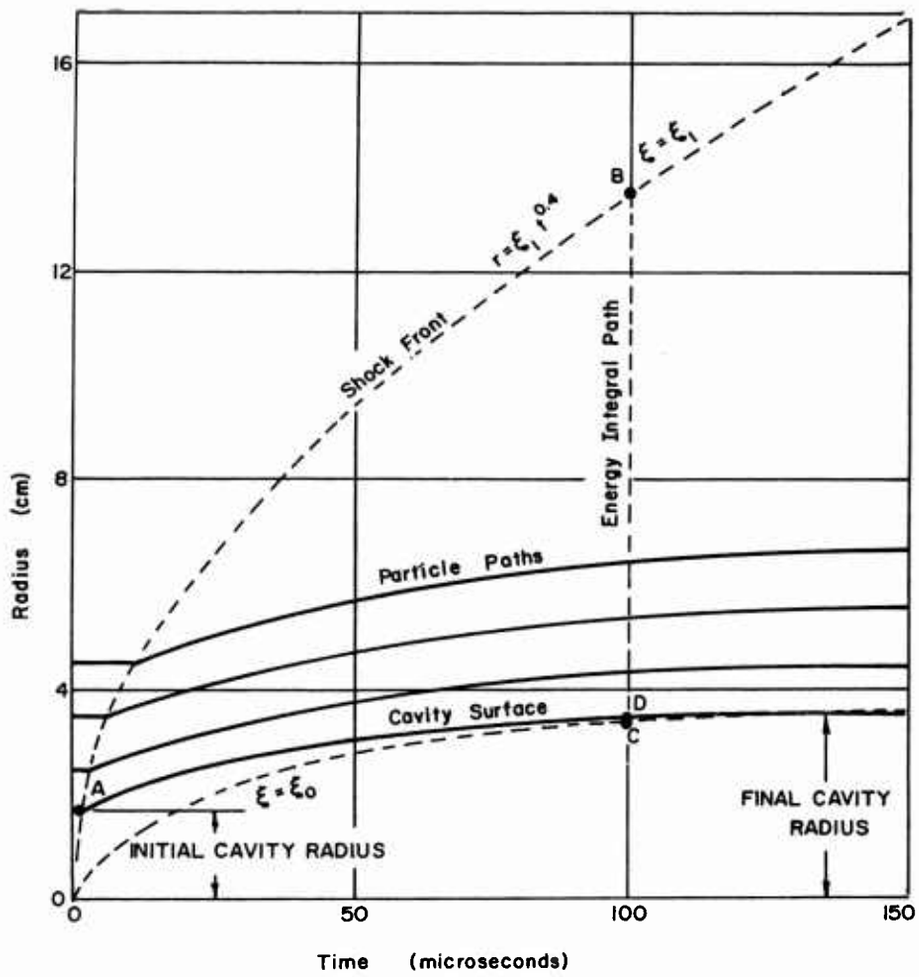

FIG. 6 - CAVITY EXPANSION AND PARTICLE TRAJECTORIES

TABLE 1

Variation of Physical Quantities Along

Solution Curve and Cavity Surface

T	U	P	ξ	D	E	R
sec x 10^{-6}				gm/cc	ergs x 10^{12}	cm
.8684	.09302	.02856	451.28	3.5182	-0.0	1.698
.9539	.09312	.02854	438.45	3.4282	-.188	1.713
1.062	.09324	.02852	424.25	3.3282	-.368	1.730
1.186	.09337	.02844	410.10	3.2282	-.520	1.748
1.329	.09352	.02846	396.02	3.1282	-.648	1.767
1.495	.09369	.02843	381.99	3.0282	-.755	1.786
1.688	.09389	.02840	368.02	2.9282	-.844	1.807
1.939	.09411	.02836	354.12	2.8282	-.918	1.828
2.181	.09436	.02832	340.29	2.7282	-.979	1.851
2.496	.09466	.02827	326.52	2.6282	-1.029	1.874
2.872	.09500	.02821	312.83	2.5282	-1.069	1.900
3.323	.09539	.02815	299.21	2.4282	-1.101	1.926
3.868	.09586	.02807	285.69	2.3282	-1.127	1.954
4.533	.09641	.02799	272.24	2.2281	-1.148	1.984
5.350	.09707	.02789	258.89	2.1282	-1.164	2.016
6.364	.09787	.02777	245.63	2.0282	-1.176	2.050
7.636	.09884	.02764	232.48	1.9282	-1.186	2.087
9.252	.10003	.02749	219.43	1.8282	-1.193	2.127
11.33	.10152	.02731	206.51	1.7282	-1.198	2.171
14.04	.10341	.02710	193.71	1.6282	-1.202	2.219
17.65	.10585	.02686	181.05	1.5282	-1.205	2.272
22.52	.10904	.02669	168.55	1.4281	-1.207	2.332
29.28	.11331	.02628	156.21	1.3282	-1.209	2.401
38.91	.11914	.02593	144.08	1.2282	-1.210	2.481
53.07	.12728	.02555	132.17	1.1282	-1.211	2.577
74.76	.13883	.02513	120.56	1.0282	-1.211	2.696
109.5	.15536	.02462	109.38	.9282	-1.212	2.849
168.3	.17866	.02384	98.85	.8282	-1.212	3.058
273.2	.21002	.02241	89.36	.7282	-1.212	3.355
470.8	.24867	.01974	81.30	.6282	-1.212	3.795
865.8	.29068	.01550	74.96	.5282	-1.212	4.465
1717	.32972	.01012	70.40	.4282	-1.212	5.514
3681	.35941	.00478	67.43	.3282	-1.212	6.968
7404	.37363	.00098	65.87	.2282	-1.212	9.257
8357	.36027	.00001	65.67	.1282	-1.212	9.687

4.4. Blast Waves in Other Metals

The study of blast waves in other metals is essentially the study of the part γ plays in the theory of self-similar motion. For this reason the present section will explore in some detail the many intricate ways that γ enters into the problem.

Selected for study were 3 common metals, copper ($\gamma = 8.5$), iron ($\gamma = 16$), and lead ($\gamma=5.9$). Figure 4 is a log-log plot of the shock wave data from Ref. 19. Straight lines were passed through the data and the slope measured to obtain the values of γ.

In the method of obtaining the solution of the differential equation (3.20), the functions U, P, D and the particle trajectories as well as shock wave paths are the same as in Sec. 4.3. All that is necessary is to change the value of γ in the computer program. (See Appendix B).

For purposes of comparison the distribution of velocity and pressure were calculated on the cavity surface and plotted in Figs. 8 and 9. An r-t diagram for the four metals is shown in Fig. 7.

Of particular interest is the fact that the γ's used range from 5.9 for lead to 16 for iron. This value used for iron is supposed to represent the lower pressure range in which iron has a body centered cubic lattice. It can be shown (Fig. 10) that for $\gamma = 7$ the shock front falls on one of the singular points of the differential equation (3.20). For this case there exists [4] a particularly simple solution of equation (3.20), i.e.,

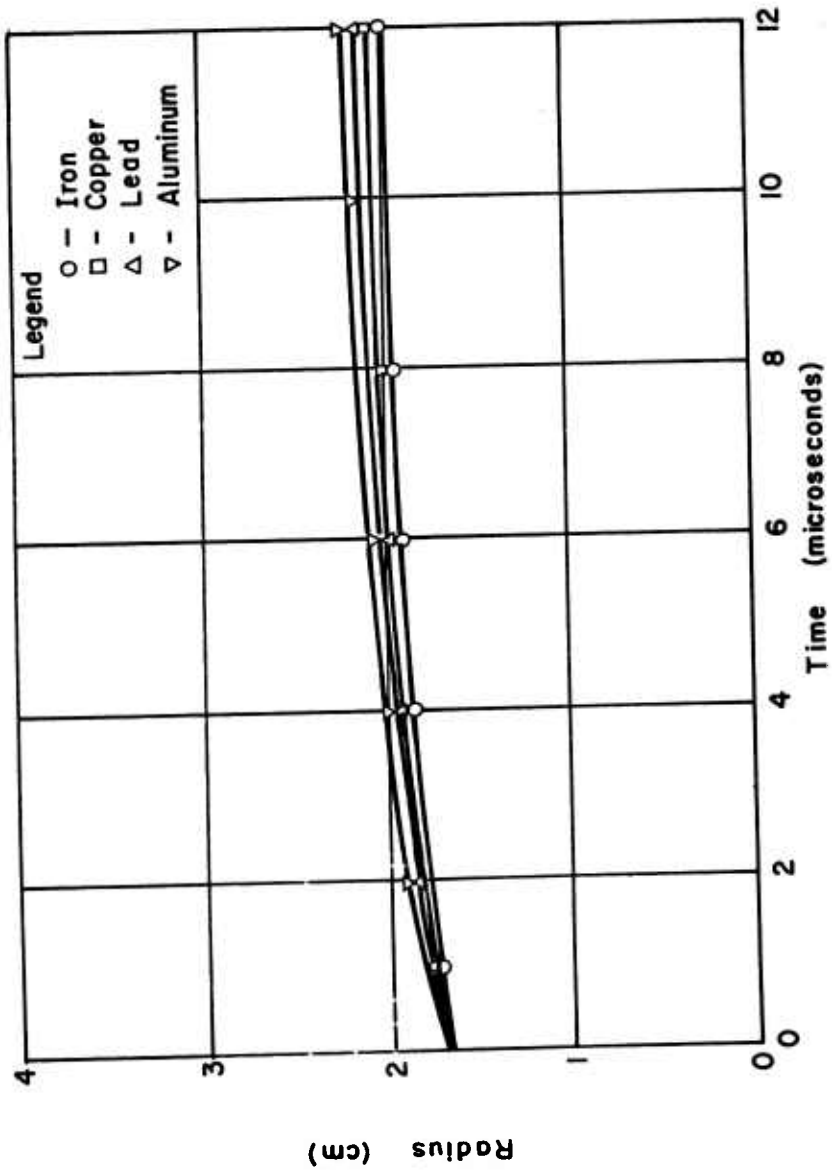

FIG. 7 – CAVITY EXPANSION FOR FOUR METALS

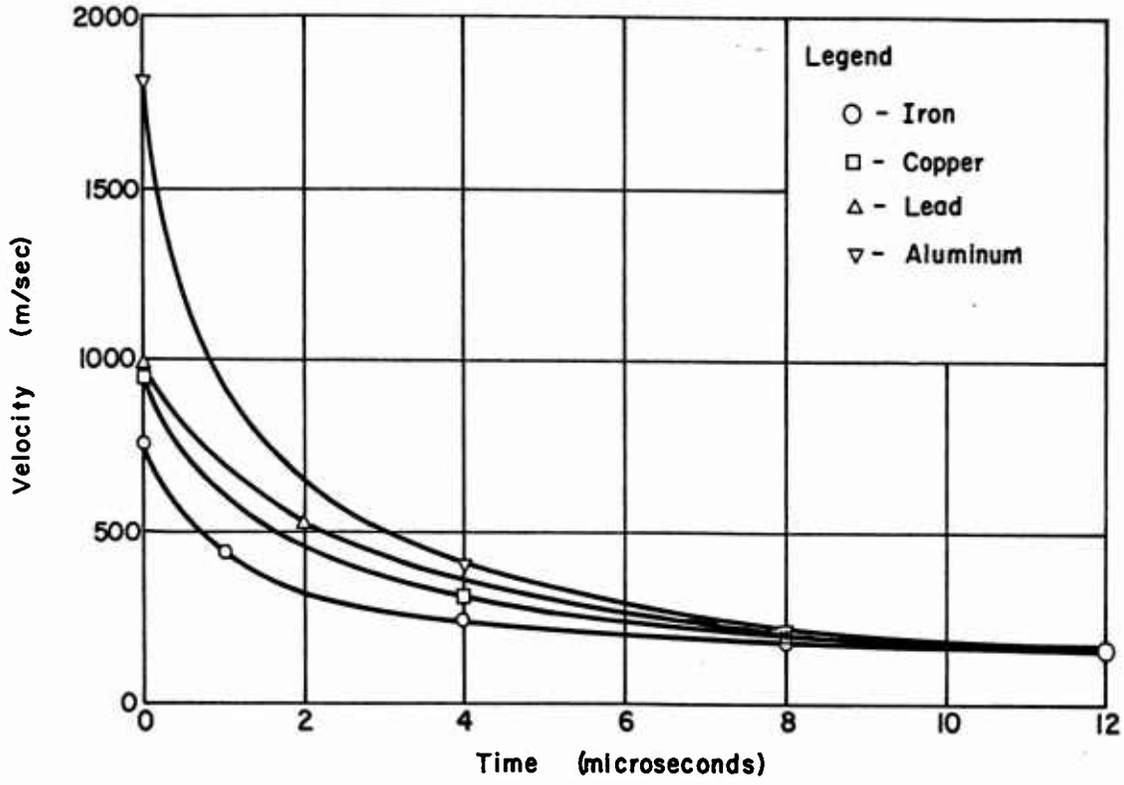

FIG. 8 - VELOCITY DECAY ON CAVITY SURFACE FOR FOUR METALS

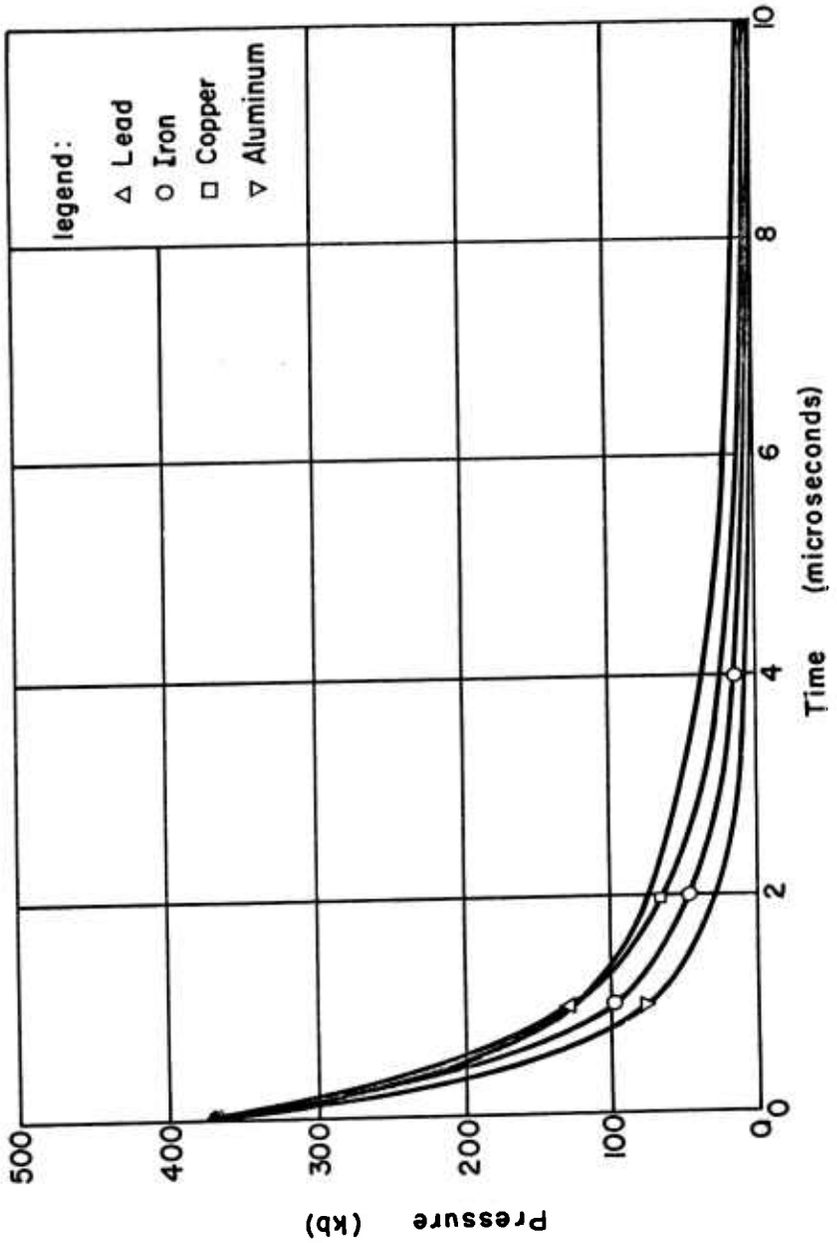

FIG. 9 – PRESSURE DECAY ON CAVITY SURFACE FOR FOUR METALS

$$u/u_2 = \xi/\xi_1 = r/R_s = \rho/\rho_2$$
$$p/p_2 = (\xi/\xi_1)^3 \qquad (4.24)$$

A value of $\gamma = 7$ serves to separate the domains of the function U. For $\gamma < 7$;

$$2/5\gamma \leq U \leq \frac{4}{5(\gamma+1)}$$

and for

$$\gamma > 7 \; ; \qquad \frac{4}{5(\gamma+1)} \leq U \leq 2/5 \; .$$

The value $U = \frac{4}{5(\gamma+1)}$ corresponds to the shock wave in a gas due to a point explosion and $2/5\,\gamma$ corresponds to the center of the explosion. However, in the cavity expansion it is meaningless and hence, lower bound of the domain of U would be some number greater than $2/5\gamma$.

For $\gamma > 7$ the domain of the function U is bounded above by $U = 2/5$ which corresponds to the edge of a so-called vacuum for a point explosion in a gas and below by the shock front. The value of $U = 2/5$ would not necessarily apply to the cavity problem. Fig. 16 shows the behavior of the solution curves for variable γ.

However, it is significant that the solution curve $P = P(U)$, which describes the process, has entirely different behavior in the two ranges. (See Figs. 10, 16). Figure 10 shows the changeover from solution curves which go to point B from those which go to D, (Fig.3).

It is fitting at this time to mention that the careful consideration of the singular points and their physical meaning came about from having the analytical solution of the strong blast wave problem. It is doubtful if this could have been accomplished by numerical computation alone. This also applies to establishing the exact domains of the function U. However, it is possible to determine the type of singular point that exists as well as a good description of the general behavior of the solution curves without the analytical solution of the differential equation.

4.5. Consideration of the Non-Similar Aspects of the Blast Wave Problem

It is well known that even for the case of spherical blast waves in air that for large time the flow becomes non-similar. That is, the motion can no longer be described by the self-similar assumptions.

This is particularly true for the case of shock waves in metals where use has been made of the strong shock approximation. For large values of time the density ratio ρ_2/ρ_1 is not constant and the shock front is no longer described by $R_s = \xi_1 t^{2/5}$. In order to extend the domain t of the self-similar solution it is necessary to account for these non-similar effects.

An approximate theory developed by Rae [10] for the cratering problem will be considered and its use in the cavity expansion problem described. The assumption is that for any shock speed $C = \dot{R}_s$ the distribution of velocity, pressure, density, etc., are the same as for the self-similar polytropic equation of state distributions which would

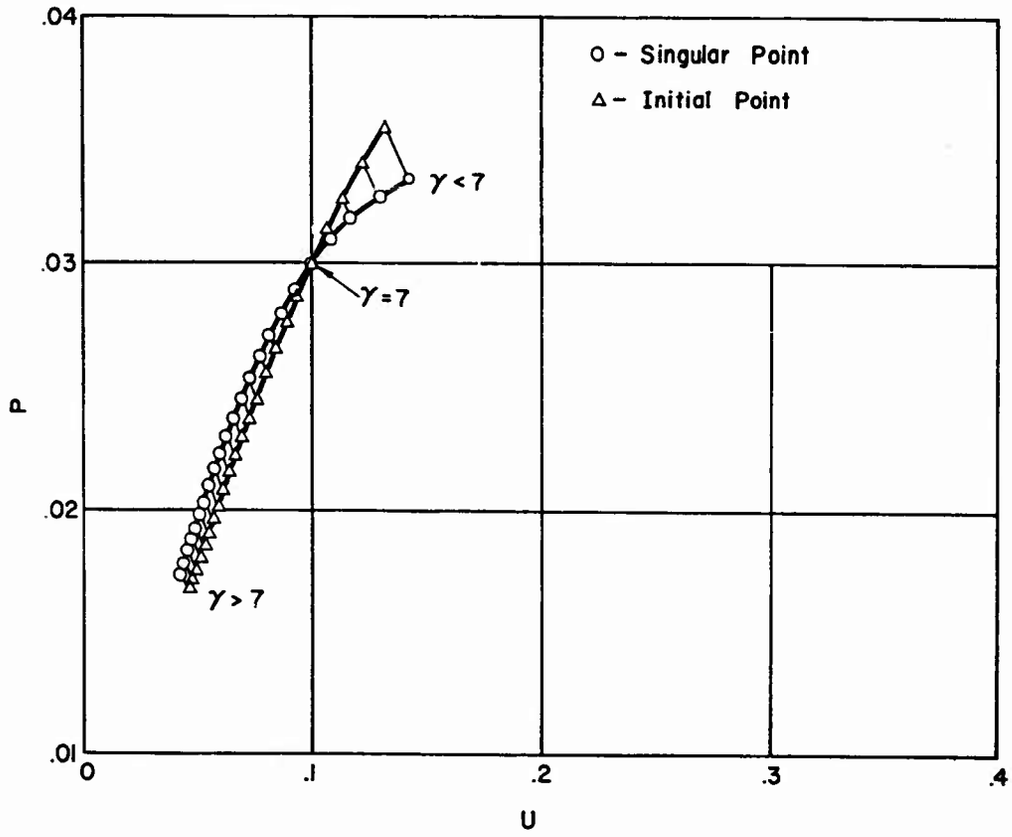

FIG. 10 – RELATIVE POSITION OF S4 AND SHOCK FRONT FOR VARIABLE γ

have the same values at the shock. This allows the density ratio ρ_2/ρ_1 to vary and thus accounts for one of the non-similar factors mentioned earlier. However, even though we have satisfied the conditions at the shock front, the flow field behind the shock is still incorrect. For the cratering problem this is shown [10] to be a fairly good approximation.

We recall that the density ratio was given by the expression

$$\rho_2/\rho_1 = \frac{\gamma+1}{\gamma-1} \quad .$$

This can be rewritten as

$$\gamma = \frac{\rho_2/\rho_1 + 1}{\rho_2/\rho_1 - 1} \tag{4.25}$$

Thus if the shock speed were such as to cause a density ratio of 1.2, then the solution is assumed to be the self-similar solution for $\gamma = 11$.

Note that as $\rho_2 \to \rho_1$ the value of γ becomes infinite. (As the shock wave decays to a stress wave $\gamma \to \infty$.)

If the shock speed $\dot{R}_s$ is considered as the independent variable, then Eq. (4.25) becomes

$$\gamma = \frac{(2S - 1)\,\dot{R}_s + c}{\dot{R}_s - c} \quad . \tag{4.26}$$

The relation $\dot{R}_s = c + Su_2$ used in this equation has been shown [22] to approximate the Hugoniots of several metals very well.

We now turn our attention to the energy integral Eq. (3.25).

$$E = \int_{R_o}^{R_s} \left(\frac{p}{\gamma+1}\right) + \frac{1}{2} u^2) \, \rho 4\pi r^2 dr$$

$$= 4\pi \int_{R_o}^{R_s} \left\{\left(\frac{r}{t}\right)^2 \frac{DP}{\gamma-1} + \frac{1}{2} \left(\frac{r}{t}\right)^2 U^2\right\} r^2 dr. \qquad (4.27)$$

but $\xi_1 = R_s t^{-\alpha}$, $\frac{dR_s}{dt} = \dot{R}_s = \alpha\left(\frac{R_s}{t}\right)$, $(\dot{R}_s)^2 = \alpha^2\left(\frac{R_s}{t}\right)^2$

also $r^2 = \xi^2 t^{2\alpha}$

Using these relations and substituting where appropriate into Eq. (4.25), we find

$$E = \dot{R}_s^2 \, R_s^3 \, F(\gamma) \quad , \qquad (4.28)$$

where

$$F(\gamma) = \frac{4\pi}{\alpha^2} \int_{\xi_o}^{\xi_1} \left(\frac{PD}{\gamma-1} + \frac{1}{2} U^2\right) \frac{\xi^2}{\xi_1} \, d\xi \quad .$$

Solving (4.27) for R_s we find

$$R_s = \left(\frac{E}{F(\gamma) \, \dot{R}_s^2}\right)^{1/3} \qquad (4.29)$$

Since γ is a function of $\dot{R}_s$ by Eq. (4.26) this expression becomes

$$R_s = \left(\frac{E}{F[\gamma(\dot{R}_s, S)]\dot{R}_s^2}\right)^{1/3} \tag{4.30}$$

Equation (4.30) describes the shock radius in terms of shock speed and is a very useful relationship. By considering E as a free parameter Eq. (4.30) could be used to fit test results. On the other hand, the expression could be solved for E and estimates could be made of the percent of available energy present in the solid.

If equation (4.30) is solved for $\dot{R}_s = \dot{R}_s(R_s)$ and the identity

$$t = \int_{R_s}^{R_s} \frac{dR_s}{\dot{R}_s} + k \tag{4.31}$$

is used, we obtain an expression for $R_s = R_s(t)$. The value of k is determined fron consideration of the "delay time" discussed in Section 4.3.

With the relations $R_s = R_s(t)$ and $R_s = R_s(\dot{R}_s)$ at our disposal it is possible to obtain the distributions of velocity pressure and density throughout the solid. The cavity radius versus time curve can also be found. However, the procedure used in Section 4.3 would have to be modified.

We recall that in solving the problem for constant γ that we constructed one solution curve $P = P(U)$ which described the functions for all ξ. In the case when γ is allowed to vary continuously, an infinite number of solution curves must be constructed.

The obvious way to avoid this is by considering small increments of time Δt at the end of which the shock speed is calculated. This value of $\dot{R}_s$ is used to calculate the corresponding γ from Eq. (4.25) and for this instant the distribution of velocity, pressure and density as well as the particle velocity on the cavity surface. This would be continued to the limit of validity of the equation of state or by using some other criterion which terminated the solution.

4.6. Summary and Conclusions

In this chapter we have attempted to study the cavity formation process in several metals by determining how the important physical variables of cavity radius, velocity, pressure, and density vary with time and position near the cavity. The most prominent general feature of the whole process is the short time of the "shock" regime as compared with the total time of the expansion. One general criterion for the end of the shock is furnished from the time when the super-sonic velocity of the shock front drops to sonic i.e., at the point P in Fig. 5, where the slope attains the value for elastic disturbances in the material. There is some concern whether the self-similar solution can be used beyond this point since it would predict a subsonic shock velocity. However, it could mean that a large plastic wave is developed which travels at a speed less than the elastic wave velocity. This transition region is highly uncertain. This situation has occurred after 0.5 microsec.

We note that the highest pressures and densities in the metal are located just behind the shock front, and trail off with decreasing

radius to minimum values at the cavity boundary. We note that the equations of state (Fig. 4) which have been used for the calculations have a lower limit of about $p = 100$ kb. This could also be used as a criterion for shock termination (point D, Fig. 5). This point is reached in 0.7 μ sec. These conditions thus determine a roughly parallelogram shaped region ODPE in the r,t-plane for the validity of the assumed theory. Note that the cavity has only expanded 0.1 cm during this period, which is about 1/30 of the total observed increase in radius. We are thus justified in referring to the shock process as impulsive, i.e., the later stages of the process are insensitive to many features of the shock part. Hence, the self-similar solution remains valid at least for the analysis of the shock zone.

The asymptotic characteristics of the solutions are thus not of direct physical interest since they do not apply to the problem much beyond the region described above. The expansion zone, headed by a wave travelling with the dilatational wave velocity goes on for at least 100 μ seconds, during most of which the metal continues to move by fluid or plastic flow.

The final cavity radius attained is of great interest to the general problem as this value is directly observable on the specimens after blast. In principle the prediction of this radius should afford a test of any theory, but the matter is not so direct as this, since several theories are involved. It is now evident that the cavity formation process is complicated. It starts under one theory (in which the state of the metal is fairly well established) but terminates in a

different state of the material, about which information is almost completely lacking. Several mechanisms have been suggested for terminating the cavity expansion:

(1) an energy-level criterion

(2) a temperature criterion

(3) a yield-point criterion

Criteria such as (2) or (3) are tempting because they tend to provide fairly definite marks as to when the material "freezes", either when a given temperature, or a given pressure is reached. However, our knowledge of materials under these conditions is still too incomplete to solve this problem. The total energy of the moving material appears to stop increasing after the expansion phase has begun, so there is no change in energy. Furthermore, any quantitative use of energy balances would require careful accounting of all the energy losses as well.

It was shown that in the self-similar approach the only difference in the approach used for different materials was the material constant γ. Also there is considerable difference in the behavior of materials whose value of γ is less than 7 compared to those having a value of γ greater than 7, due to the completely different behavior of the solution curve. (See Fig. 10) One must be reminded that these comparisons are valid only under the assumption that the equation of state used in this analysis is valid in the stated range of pressures.

In the previous section a procedure was discussed for extending the regime in which a self-similar type solution is valid.

Application of this theory to the problem of cavity expansion in metals was described in some detail without presenting numerical results.

In considering the application of this theory to other materials, the only difference to be encountered would be the initial value of γ used.

CHAPTER V

EXPERIMENTAL PROCEDURE AND RESULTS

5.1. Description of Specimens and Experimental Arrangement

The experiments reported on in this chapter were performed at the Ballistic Research Laboratories of Aberdeen Proving Grounds, Aberdeen, Maryland. The writer acted as an advisor on the test program and participated to a minor extent in the testing. Some of these results will appear in a joint paper [23] with a member of the Ballistic Research Laboratories staff to be published later.

The specimens chosen for the tests were spheres made of 24 ST and 6061-T4 aluminum alloys. The first series of tests were made using spheres whose outer diameter was nominally eighteen centimeters. The second series was made using spheres of 25 cm outer diameter. The inner cavity in both cases was 3.4 centimeters. (See Fig. 11). The exact dimensions are given in Table 2. A threaded well was machined in the spheres in which a threaded plug with a hemispherical cup machined in the end was inserted. This arrangement offered essentially a condition of an isolated cavity inside a metal sphere. A small diameter hole drilled through the axis of the plug provided a means for running the firing line and ionization probe to the cavity. The end opposite the hemispherical cup protruded from the sphere and served as a means of mounting the specimen.

The explosive used was a 32 gram sphere of Pentolite which fitted snugly into the cavity in the aluminum sphere.

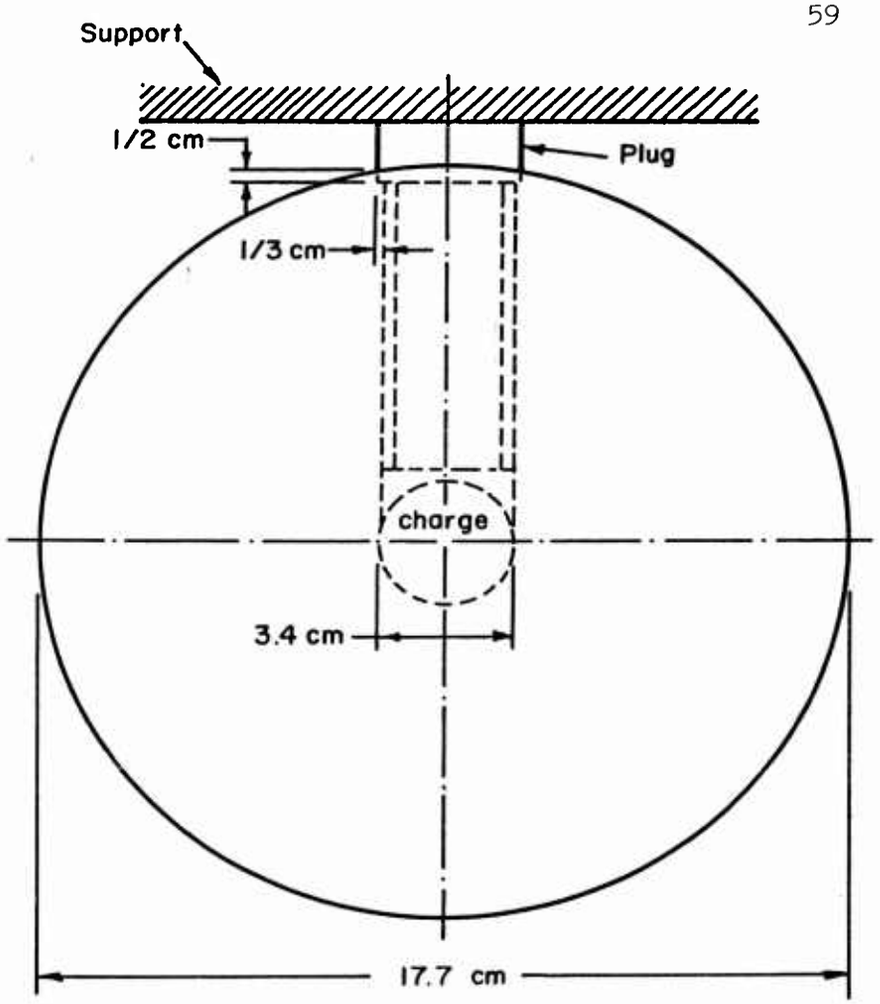

FIG 11 – SMALLER SPHERE – PRE SHOT

TABLE 2

Specimen Physical Measurements

Observations	Test Numbers 1	2	3	4	5	6*	7	8
Material	24ST	6061-T4	6061-T4	24ST	6061-T4	6061-T4	6061-T4	6061-T4
Explosive Weight, (gm)	32	32	32	32	32	32	32	32
Pre-Test Sphere Diam., (cm)	16.633	17.767	17.762	17.691	17.737	17.780	25.384	25.384
Post-Test Sphere Diam., (cm)	17.962	18.168	18.135	18.000	18.156	-	25.585	25.594
Pre-Test Cavity Diam., (cm)	3.396	3.396	3.396	3.396	3.396	3.396	3.396	3.396
Post-Test Cavity Diam., (cm)	5.946	5.956	5.842	5.890	6.678	-	7.511	7.249

*Specimen Failed

The permanent deformation of the inner and outer surface of the sphere as well as the material damage were of primary concern in the experiment. However, there were other quantities that were of great interest such as free surface velocity time curves, time of arrival of first disturbance and maximum deflection and shock velocity time curve through the material.

Two condenser type micrometers were used to obtain the free surface velocity and maximum radial deflection. These micrometers consist of a condenser arrangement in which the surface of the sphere constitutes the ground side and the other plate is placed a few tenths of a centimeter away. (See Fig. 12). The output of these micrometers is recorded on cathode ray oscilloscopes which are triggered by a simple ionization probe inserted through the plug into the explosive detonator cavity.

Quartz disc crystals are affixed to aluminum rods and threaded into the sphere to varying depths to measure the time of arrival of the disturbance through the aluminum sphere. The output from the crystals is recorded in the same way as the condenser micrometers.

After the apparatus is assembled the condenser micrometers are calibrated remotely. The explosive is then initiated and the scope traces recorded with still cameras using polaroid film.

5.2. Test Results

Table 2 contains a tabulation of pre-shot and post-shot physical measurements of each specimen. The inner cavity and outer surface measurements are averages and do not reflect the asymmetric deformation

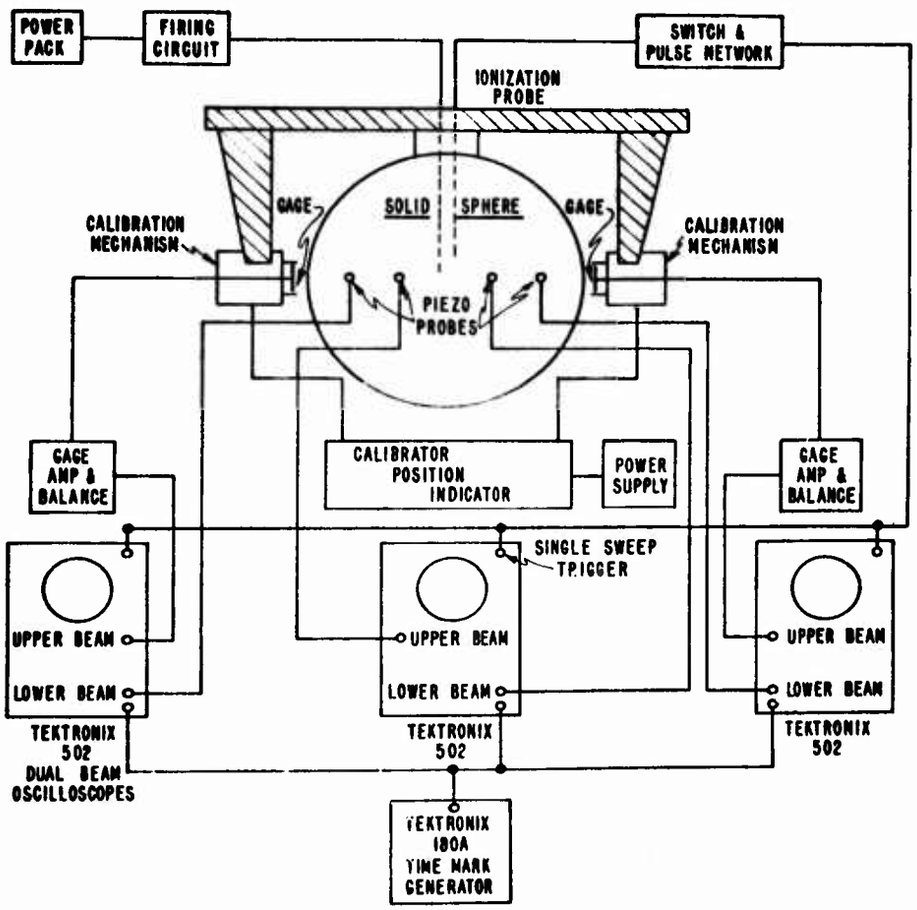

FIG. 12 EXPERIMENTAL ARRANGMENT

detected in the post-shot measurements. However, the values obtained from the recorded data presented in Table 3 do reflect this non-uniform deformation. The values in Table 2 indicate that the average increase in the outer diameter of the small spheres is about 2% and about 1% for the larger spheres. For the inner cavity the post-shot diameter was found to be about 75% greater than the pre-shot diameter for the smaller spheres. The increase for the larger spheres is, however, greater than 100%. In Table 3 we see the values of the wave velocity agree well with the known elastic wave velocity in the aluminum. It is also evident that the free surface velocity for the two materials is appreciably different.

Figure 13 shows a typical plot of data showing the response of an 18 cm sphere recorded through a condenser micrometer. Notice the definite tendency toward oscillation of the outer surface. Figure 14 is an actual trace of the surface response of the 25 cm sphere recorded by the polaroid camera.

5.3. Discussion and Conclusions

One of the most significant questions that we hoped the experiments would answer was how much the cavity size was influenced by the location of the outer boundary. More specifically, how large the sphere had to be to be considered an infinite medium. This was not answered quantitatively, but it was found that the location of the boundary was a significant factor. We notice that the post-shot cavity was consistently larger for the 25 cm sphere when compared to the 18 cm sphere. This might be explained through a coupling effect between the reflect-

TABLE 3

Data as Determined from Capacitance Gages

		Test Numbers							
		1	2	3	4	5	6	7	8
Material		24ST	6061-T4	6061-T4	24ST	6061-T4	6061-T4	6061-T4	6061-T4
Average Wave Velocity, (cm/μs)		.59	.60	.48	-	.47	.60	.58	.62
Free Surface Velocity, (cm/μs)	No. 1 gage	.37	.12	.18	.37	.18	.29	.15	.11
	No. 2 gage	-	-	.18	.26	-	.34	.14	-
Maximum Radial Expansion, (cm)	No. 1 gage	8.960	9.107	9.063	9.003	9.075	-	12.839	12.808
	No. 2 gage	-	-	9.082	9.074	-	-	12.829	12.195

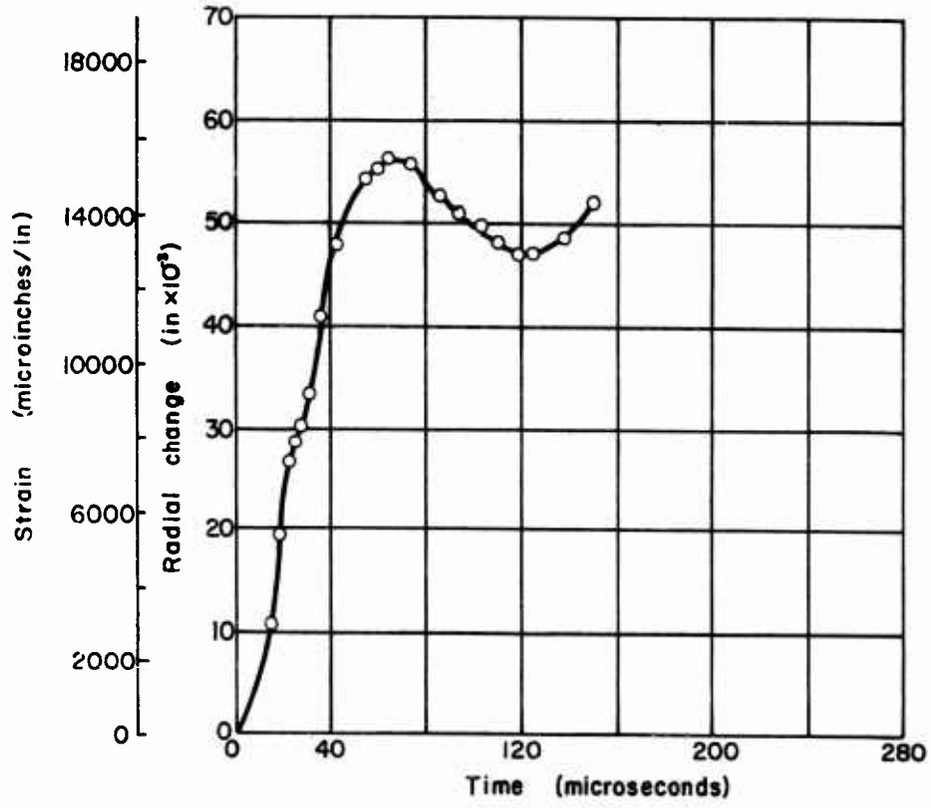

FIG. 13 - RESPONSE OF CAPACITANCE GAGE FOR SMALLER SPHERE

ed elastic wave and the plastic loading or unloading wave. Another possible explanation is based on assuming that the motion is quasi-static and fully plastic. Hill [24] shows that the displacement of the inner surface increases with an increase in outer radius.

Figure 15 is a sketch of a post-shot section of the sphere. Notice the three regions marked on the sketch labeled A, B, C. Section C is a narrow region surrounding the cavity in which there are few cracks and during deformation the metal appears to flow much as a fluid. In region B the material exhibited many small shear and tension failures. Zone A appeared to be dominated by reflective effects and showed several "scabbing" type failures.

In all of the tests, the plug was blown out. It was concluded that this did not effect the final cavity size significantly as the sphere had to expand throughout to free the plug. However, the presence of the plug was concluded to cause the asymmetric deformation of the sphere.

The quartz disc crystals used to signal the time of arrival of the wave were only able to measure the small amplitude waves. The crystals would not sustain the violent conditions in the shock zone.

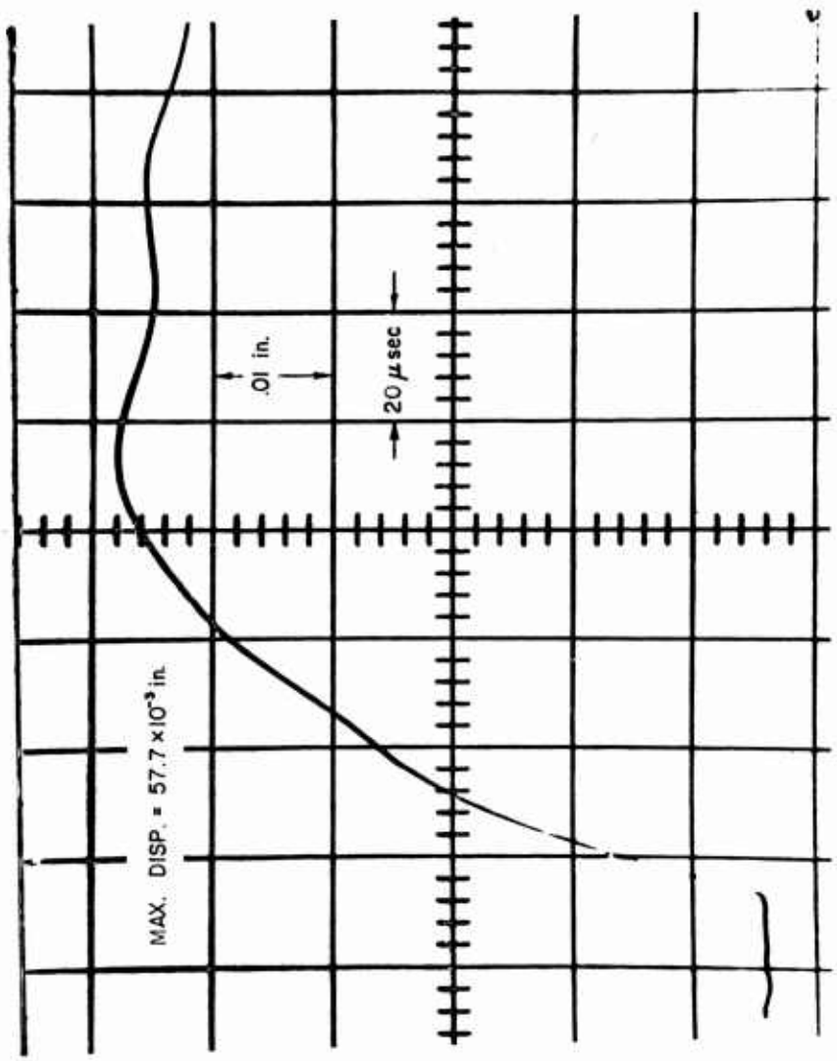

FIG. 14 – RESPONSE OF CAPACITANCE GAGE FOR LARGER SPHERE

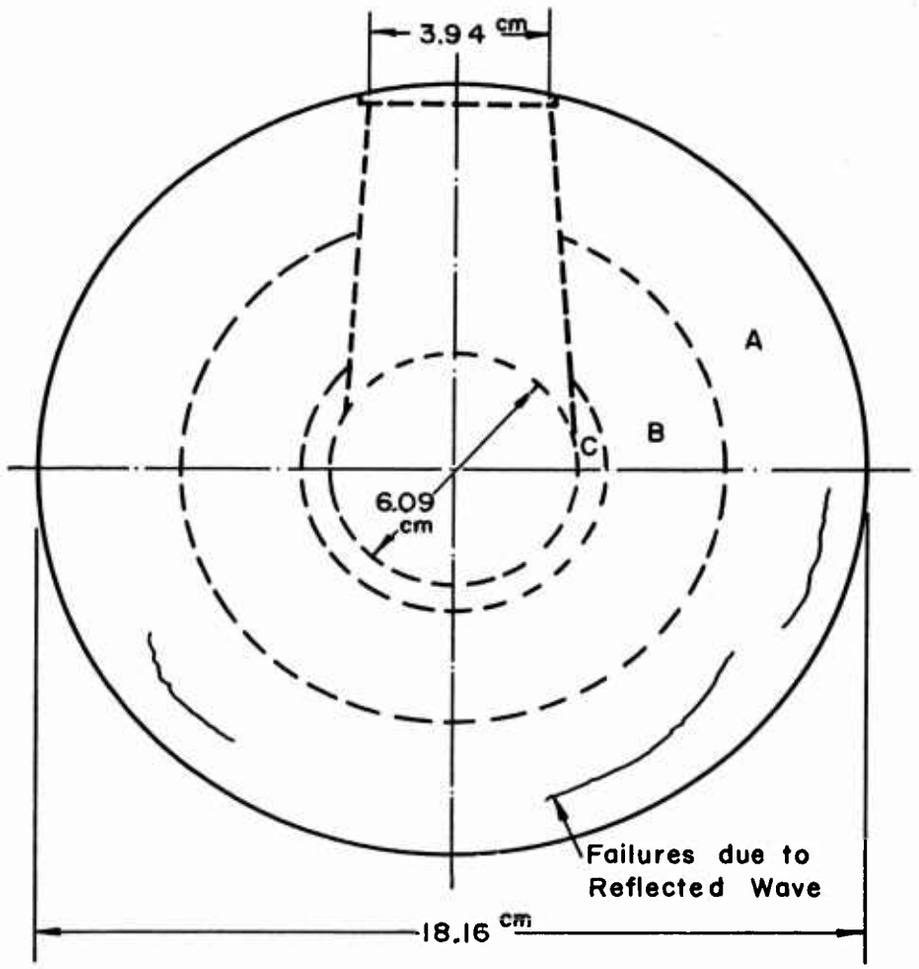

Zone A – No damage, other than that of reflected wave

Zone B – Heavily damaged

Zone C – "Fluid" zone

Note – Dimensions are approximate

FIG.15 – SMALLER SPHERE – POST SHOT.

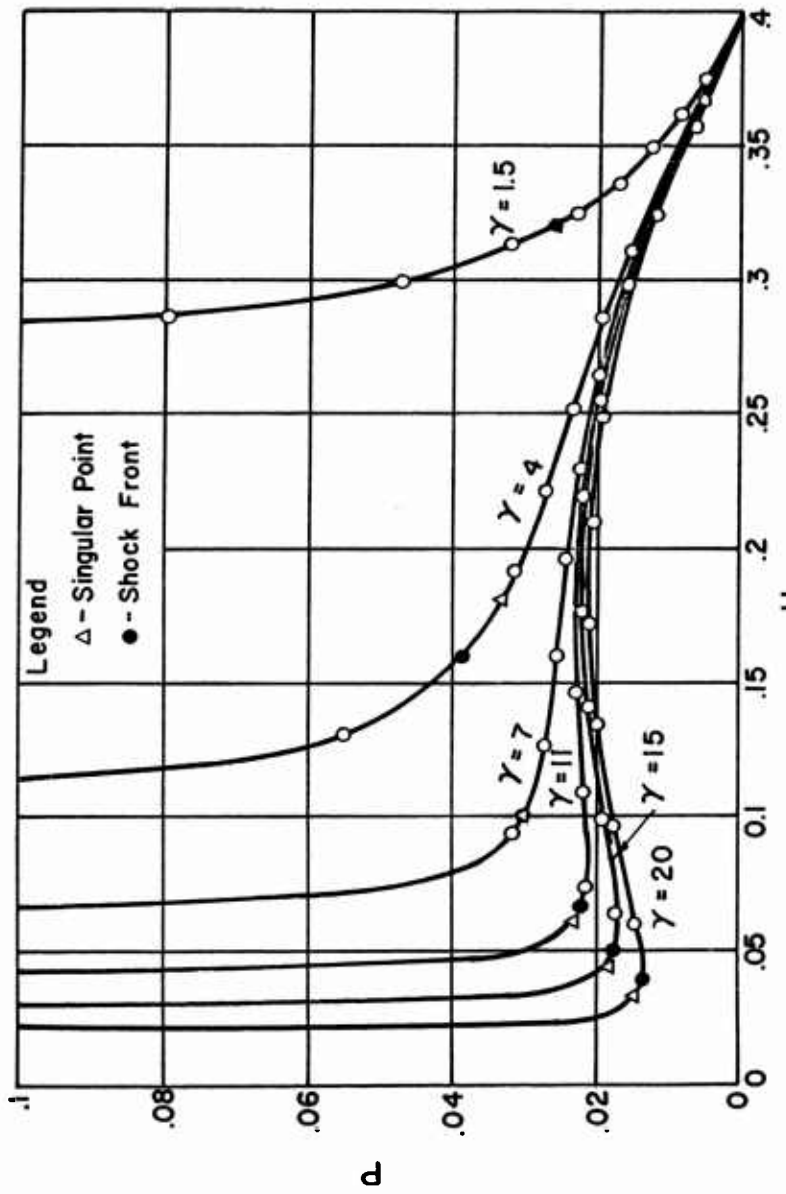

FIG. 16 - BEHAVIOR OF SOLUTION CURVE FOR VARIABLE γ

CHAPTER VI

CLOSURE

6.1. Summary and Conclusions

The behavior of shock waves in metals is a subject of current scientific and engineering interest. There has been a considerable amount of experimental research and a lesser amount of analytical effort in this field. Some of the most successful approaches to the problems of shock waves in solids have been based on the so-called "hydrodynamic" model.

In Chapter III of this thesis the theory of self-similar motion is reviewed and discussed. The equations for spherical motion of a compressible inviscid fluid subjected to a strong shock are solved.

One of the main contributions of this thesis is contained in Chapter IV. In this chapter the problem of the dynamic short time behavior of a ductile metal surrounding a spherical detonated charge of high explosive, is solved for the first time. The problem is approached using the theory of self-similar motion presented in Chapter III. The trajectories of the shock waves and cavity surface are obtained as well as values for the variation with time of pressure and velocity on the cavity surface. Cavity formation in other metals is discussed and values for shock and cavity surface trajectories are obtained. Pressure and velocity variation with time on the cavity surface are also presented.

A critical analysis of the theory of self-similar motion as it applies to shock waves in solids is presented. The restrictions im-

posed on its use by equations of state and assumptions of constant shock strength are discussed. An equation of state called quasi-polytropic is considered and its incompatibility with the theory of self-similar motion exhibited.

A method which accounts for one of the non-similar aspects encountered at large times for spherical shock waves in solids is discussed and its application to the cavity expansion problem outlined.

The results of the analysis for aluminum show that the "shock zone" or range of validity of the self-similar solution is very small. The reasons for this are (1) after only 0.5 microseconds the shock wave velocity predicted by the self-similar solution has fallen to that of the elastic wave velocity in the material, (2) in only 0.7 microseconds the pressure behind the shock front has fallen to 100 kb (which has been chosen as the lower bound for the range of validity of the equation of state of aluminum). At this time the cavity has expanded 0.1 cm which is only 1/30 of the total increase in radius.

Thus the material behavior is referred to as impulsive, that is, the latter stages of the process are insensitive to many of the features of the shock part.

The final cavity radius attained is of great interest to the general problem as this value is directly observable on the specimen after blast. In principle, the prediction of this radius should afford a test of any theory, but the matter is not so direct as this, since several theories are involved. It is now evident that the cavity formation process is complicated. It starts under one theory, in which the state of

the metal is fairly well established, but terminates under another, about which there is little information.

In applying the theory of self-similar motion to cavity expansion in other metals, it is seen that the only difference is the material constant γ. The behavior of the solution curves for variable γ is shown in Fig. 16. For $\gamma = 7$ the solution is particularly simple (see Eqs. (4.24)).

In considering the application of the theory, which takes into account the variable density ratio across the shock front (see Sec. 4.5), we see that a numerical approach can be successfully used to extend the self-similar theory.

In Chapter V the results of new experiments were presented. These studies were made for the purpose of verifying the foregoing theory. Aluminum spheres of 18 cm and 25 cm diameter were subjected to an internal blast from a 32 gm spherical charge of Pentolite. The resulting surface motion and permanent deformation were presented and the effect of the size of the sphere established.

The inner cavity of the smaller spheres was deformed from an initial diameter of 3.40 cm to 6.0 centimeters. The cavity of the larger spheres, however, increased from a diameter of 3.4 to 7.4 cm.

Other pertinent data is given in Tables 2 and 3.

The actual cause of the difference in cavity size is not known. However, the possibility of coupling of the waves due to reflection from the boundaries is a possible explanation. Another possible cause is that presented by Hill [24] in which the motion is assumed quasi-

static and the sphere completely plastic. Under these assumptions Hill shows that the inner radius increases with the outer radius, other things remaining equal.

The damage suffered by the spheres is seen to be rather sharply delineated into 3 categories. The first is the zone immediately next to the cavity. In this zone there were few shear cracks and the material appeared to have been deformed in a fluid-like manner.

In the second zone this was not the case. There were numerous shear and tension cracks and damage was severe.

The outer zone was dominated by reflective effects. Most of the failures in this zone were "scabbing" type failures.

Another interesting fact determined from the experiments is that there is definitely some oscillation of the sphere.

In all the tests the plug was blown out. It was decided that this did not affect the cavity size to a great extent, since it only occurred after the sphere had expanded sufficiently to allow its release.

6.2. Suggestions for Further Research

It is obvious in considering the analysis of later stages of the cavity expansion process that a criterion is needed for marking the end of the self-similar solution.

Several such mechanisms have been suggested such as temperature, material strength [10] and energy [9] but none are completely satisfactory.

To obtain a better approximation of the actual material behavior for later time, one must account for the non-similar aspects of the

flow. For this reason it is suggested that some numerical results be obtained using the theory described in Section 4.5.

In order to obtain an exact analytical solution, the boundary conditions on the inner cavity surface must be prescribed for all values of time. This will require a detailed analysis of the effect of confinement on the detonation pressures of the explosive, and also consideration of pulsation of the exploded gas.

There remains the problem of defining the equation of state of a solid throughout the range of pressures encountered in the blast wave problem. This problem is complicated by phase changes and other complicated mechanical behavior. This should continue to be an area of great effort.

There are several questions that can be answered by experimental investigations which would facillitate the formulation of a satisfactory theory.

(1) What part do the reflected waves play in the final cavity size. This could be answered using a flash x-ray or some similar device.

(2) What is the actual initial detonation pressure exerted on the metal.

There is need for a pressure sensing device which will survive the extreme conditions experienced in this test.

(3) How much time is required for the cavity to assume its final configuration.

APPENDIX A

SINGULAR POINTS OF ORDINARY DIFFERENTIAL EQUATIONS

The singular points of an ordinary differential equation $dv/dx = f(x,v)/g(x,v)$ are defined to be those points for which $dv/dx = \frac{0}{0}$.

It is necessary to study carefully the singular points of the differential equation (Eq. (3.20)), $\frac{dP}{dU} = \frac{P[N(U) + PQ(U)]}{R(U) + PS(U)}$, in order to construct solution curves using numerical methods.

Poincare showed that the differential equation

$$\frac{dv}{dx} = \frac{ax + bv + f_2(x,v)}{cx + dv + g_2(x,v)} \tag{A.1}$$

in which the constants a, b, c, d are such that $\Delta = ad - bc \neq 0$ and in which f_2 and g_2 vanish like $x^2 + v^2$ as $x,v \to 0$, has as its only singularities those of the much simpler equation

$$\frac{dv}{dx} = \frac{ax + bv}{cx + dv} \quad . \tag{A.2}$$

It is obvious that these occur only at the origin $(x,v) = (0,0)$. However, in order to study a singular point (U_o, P_o) a change of variables can be made by letting $x = U - U_o$, $v = P - P_o$. Thus in the neighborhood of an isolated singularity (U_o,P_o) the differential equation (3.20) can be written $\frac{dv}{dx} = \frac{ax + bv}{cx + dv}$. The behavior of the solution curves in the neighborhood of the point is then determined by the values of a, b, c, d.

The singular points of Eq. (3.20) will now be determined and classified according to the notation and criterion of Stoker [25]. Rewritting Eq. (3.20)

$$\frac{dP}{dU} = \frac{P[N(U) + PQ(U)]}{R(U) + PS(U)} \qquad (A.3)$$

By inspection of Eq. (A.3) we find

(S1) $U = 0$, $P = 0$

(S2) $U = \alpha$, $P = 0$

(S3) $U = 1$, $P = 0$

The location of (S4) is determined by the condition

$$\frac{N(U)}{Q(U)} = \frac{R(U)}{S(U)} = - P \quad .$$

This statement leads to the cubic equation

$$A_3 U^3 + A_2 U^2 + A_1 U + A_o = 0$$

where

$$A_3 = 2\gamma (1 - 3\gamma)$$

$$A_2 = 3\gamma^2 (3\gamma - 1) + \gamma(7 - 5\alpha) - \gamma(3\delta + 4\beta) + \delta + 2\beta$$

$$A_1 = \gamma (3\alpha\delta + 6\alpha\beta - 2\beta - 4\alpha) + (2 - \alpha) (\delta + 2\beta)$$

$$A_o = - 2\alpha (\delta + 2\beta)$$

For aluminum ($\gamma = 7.6$) the point (S4) is given by $U = 0.0916$, $P = 0.02884$. The remaining roots are imaginary.

A summary of the results of the classification of the nodes is as follows:

Singular Point		Classification
S1	(0,0)	stable node
S2	(α,0)	saddle point
S3	(1,0)	stable node
S4	(.0915, .02884)	unstable node

From numerical calculations it appeared that the solution curve for $\gamma = 7.6$ should end at S2. However, this was a saddle point of the differential equation and curves starting near S4 never went into S2. (Theoretically we know there is only one curve which does so and this cannot be found numerically.) In order to obtain a better approximation to a solution curve joining the points S2 and S4 the following procedure was used.

Near $U = \alpha$ we have

$$P = P_o + \left(\frac{dP}{dU}\right)_{U=\alpha} (U - \alpha) + \ldots \qquad (A.4)$$

Dividing both numerator and denominator in the differential equation (A.3) by $U - \alpha$ and putting

$$m = P/_{U-\alpha} \qquad (A.5)$$

we may write

$$\frac{dP}{dU} = m \frac{[N(U) + m\,(2\beta + 2\gamma(U - \alpha))]}{U(1-U) + (2\beta + 3U\gamma)m} \qquad (A.6)$$

We now seek a solution curve which approaches the point $U=\alpha$ with a definite limiting slope (i.e. be locally a straight-line). Letting $U \to \alpha$ in Eq. (A.6), placing the resulting expression in (A.4), and dividing by $(U-\alpha)$, we obtain the following equation for m:

$$m = m \frac{[N(U) + m\,(2\beta + 2\gamma\,(U - \alpha))]}{U(1-U) + (2\beta + 3U\gamma)m} \qquad (A.7)$$

Equation (A.7) has the following three solutions:

1) $m = \infty$

2) $m = 0$

3) $m = (\alpha-1)/3$

Thus there are three solution curves which pass through the point. The first two are the straight lines $U = \alpha$, $P = 0$ respectively, which are singular to the differential equation. The remaining slope is $m = -0.2$ for $\alpha = 0.4$.

By proceeding along the straight line of slope m a short distance toward $S4$ and using this point as the starting point for the numerical calculation, a very close approximation to the actual curve is obtained.

APPENDIX B

NUMERICAL PROGRAM

The problem programmed for the computer was to obtain the trajectory of the shock front and particle paths as well as distribution of physical variables from the differential equation and a starting point, (see Appendix A) together with boundary conditions and kinematic relations.

In order to avoid the difficulties caused by vertical or horizontal tangents, the differential equation (A.3) was written in the following parametric form,

$$\frac{ds}{\sqrt{P^2(N+PQ)^s + (R+PS)^2}} \quad (R + PS) \quad = \quad dU \qquad (B.1)$$

$$\frac{ds}{\sqrt{P^2(N+PQ)^2 + (R+PS)^2}} \quad P(N+PQ) \quad = \quad dP \qquad (B.2)$$

where

$$ds = \sqrt{dP^2 + dU^2} \quad = \quad \sqrt{1 + \left(\frac{dP}{dU}\right)^2}\ dU \qquad (B.3)$$

Expressions (B.1) and (B.2) are well behaved except at S4 and S2, which are carefully avoided.

The accuracy of the calculation is seen to depend on the choice of ds (other things remaining fixed). However, ds has no physical mean-

ing and the density was decided to be a better parameter. Using the relation

$$dD = - D\left[\frac{(R+PS) + 3U((U-\alpha)^2 - P)}{U - \alpha}\right] \frac{ds}{\sqrt{(N+PQ)^2 P^2 + (R+PS)^2}}$$

a program was developed where the density is the independent variable and a physical constraint was maintained on the integration.

TABLE 4

Program Symbol Table

Program Symbol	Our Notation or Name	Mode
A	α	FLT
B	β	"
C	δ	"
G	γ	"
U	U	"
P	P	"
DS	ds	"
X	ξ	"
D	ρ	"
IMAX	num. of iterations	FIX
EP	potential energy	FLT
EK	kinetic energy	"
E	E(t)	"
FN	N(U)	"
FQ	Q(U)	"
FR	R(U)	"
FS	S(U)	"
FT	P(N+PQ)	"
FW	R+PS	"
FX	$ds/\sqrt{P^2(N+PQ)^2+(R+PS)^2}$	"
DP	dP	"
DU	dU	"
FY	$(U-\alpha)^{\gamma}-\gamma P$	"
DX	$d\xi$	"
DD	$d\rho$	"
PD	$P\rho$	"
DEP		"
DEK		"
DO	ρ_1	"
R	R	"
St.47	initial U	"
St.48	initial P	"
St.54	initial ρ	"
EX	$1/\alpha$	"
T	t	"
V	u	"
Pres	p	"
DT	dt	"

TABLE 5 - FORTRAN PROGRAM

```
     COMPILE   RUN  FORTRAN
C      R-T CALCULATION PROGRAM
  100 DIMENSION IDENT(2)
    1 READ 800,A,B,C,G,DO,IDENT
  800 FORMAT(5F10.0,2A5)
    2 READ 801,X,R,DD,IMAX,PRES
  801 FORMAT(3F10.0,I10,1F10.0)
    3 IF(IMAX)44,44,4
    4 PRINT 802
  802 FORMAT(1H1,40X,32HBRL-PA.STATE PROJECT BLAST WAVES/
     11H0,48X,15HR-T CALCULATION/
     11H0,15X,10HINPUT DATA)
    5 PRINT 803,IDENT,G,R,DO,PRES,IMAX,DD
  803 FORMAT(1H0,10X,11HMATERIAL = ,2A5/
     11H0,10X,8HGAMMA = ,1F5.2/
     11H0,10X,17HINITIAL RADIUS = ,1F5.3,3H CM/
     11H0,10X,18HINITIAL DENSITY = ,1F5.3,6H GM/CC/
     11H0,10X,19HINITIAL PRESSURE = ,1F5.1,9H KILOBARS/
     11H0,10X,20HNO. OF ITERATIONS = ,1I4/
     11H0,10X,20HDENSITY INCREMENT = ,1F6.3,6H GM/CC//
     11H0,1X,1HI,7X,1HT,11X,1HR,12X,1HV,12X,7HPRES KB,9X,1HD,11X,1HU, 1 1X
     1,1HP,9X,1HX,11X,1HE//)
    6 U=A*(1.0-(G-1.0)/(G+1.0))
    7 P=(A*A*(G-1.0)/(G+1.0))*(1.0-(G-1.0)/(G+1.0))
    8 D=(G+1.0)/(G-1.0)*DO
    9 EP=0
   10 EK=0
   11 E=0
   12 DO 42   I=1,IMAX
   13 FN=G*U*(3.0*A-1.0-2.0*U)+(3.0-A)*U-2.0*A
   14 FQ=(2.0*B-(G-1.0)*C)/(U-A)+2.0*G
   15 FR=U*(U-A)*(1.0-U)
   16 FS=C+2.0*B+3.0*U*G
   17 FT=P*(FN+P*FQ)
   18 FW=FR+P*FS
   19 FY=(U-A)*(U-A)-G*P
   20 FX=-DD*(U-A)/(D*(FW+3.0*U*FY))
   21 DP=FT*FX
   22 DU=FW*FX
   23 EX=1.0/A
   24 T=(R/X)**EX
   25 DX=X*FY*FX
   26 V=R*U/T
   27 PRES=(R/T)**2*P*D*(10.0**(-9))
   28 PRINT 804,I,T,R,V,PRES,D,U,P,X,E
  804 FORMAT(1H ,I4,1E12.4,1F12.7,1E14.5,1F14.5,4F12.5,1E15.5)
   29 DT=DX/((-A/T+V/R)*X)
   30 IF(P)43,31,31
   31 T=T+DT
   32 R=R+V*DT
   33 U=U+DU
   34 P=P+DP
   35 X=X+DX
   36 D=D+DD
   37 DEP=4.0*3.141593*P*D*(X**4)*DX/(G-1.0)
   38 DEK=4.0*3.141593*(U*U)*D*(X**4)*DX/2.0
   39 EP=EP+DEP
   40 EK=EK+DEK
   41 E=EP+EK
   42 CONTINUE
   43 GO TO 1
   44 STOP
   45 END
```

BIBLIOGRAPHY

(1) Hopkins, H.G., "Dynamic Expansion of Spherical Cavities in Metals," Progress in Solid Mechanics Vol. 1, North Holland, 1960.

(2) Hunter, S.C., Proc. Conf. Properties of Materials at High Rates of Strain. London, 1960.

(3) Taylor, G.I., "The Formation of a Blast Wave by Very Intense Explosion, I, Theoretical Discussion," Proc. Roy. Soc. Lond. (A) 201, 1950, 159-174.

(4) Sedov, L.I., Similarity and Dimensional Methods in Mechanics, Academic Press, 1959.

(5) Taylor, J.L., "An Exact Solution of the Spherical Blast Wave Problem," Phil. Mag. 46, 1955, 317-320.

(6) Latter, R., "Similarity Solution for a Spherical Shock Wave," Journal of Applied Physics, 26, 1955, 954-960.

(7) Sakurai, A., "On Exact Solution of the Blast Wave Problem," Journal Physical Society, Japan 10, 1955, 827-838.

(8) Courant, R. and Friedrichs, K., Supersonic Flow and Shock Waves, Interscience Publishers, 1948.

(9) Davids, N. and Huang, Y.K., "Shock Waves in Solid Craters," Journal of the Aerospace Sciences.

(10) Rae, W.J. and Kirchner, H.P., "A Blast Wave Theory of Crater Formation in Semi-Infinite Targets," Proc. of Sixth Hypervelocity Impact Symposium, Cleveland, Ohio, 1963.

(11) Goldstine, H.H. and von Neumann, J., "Blast Wave Calculation," Communications on Pure and Applied Mathematics Vol. 8, 1955, 327-353.

(12) Brode, H.L., "Numerical Solutions of Spherical Blast Waves," Journal of Appl. Phys. Vol. 26, No. 6, 1955.

(13) von Neumann, J. and Richtmyer, R.D., "A Method for the Numerical Calculation of Hydrodynamic Shocks," Journal of Applied Physics, Vol. 21, 1950, 232-237.

(14) Lax, P.D., "Weak Solutions of Non-Linear Hyperbolic Equations and Their Numerical Computation," Communications on Pure and Applied Mathematics, Vol. 7, 1954, 159-192.

(15) Bjork, R.L., "Analysis of the Formation of Meteor Crater, Arizona: A Preliminary Report," Journal of Geophysical Research, 66, 1961, 3379-3387.

(16) Bjork, R.L., "Effects of a Meteroid Impact on Steel and Aluminum in Space," Tenth International Astronautical Congress Proceedings, Vol. II, Springer Verlag, 1960, 505-514.

(17) Walsh, J.M. and Tillotson, J.H., "Hydrodynamics of Hypervelocity Impact," Proc. of Sixth Hypervelocity Impact Symposium, Cleveland, Ohio, 1963.

(18) Eichelberger, R.J. and Gehring, J.W., "Effects of Meteroid Impacts on Space Vehicles," American Rocket Society Journal, 32, No. 10, October 1962, 1583-1591.

(19) Walsh, J.M., Rice, M.H., McQueen, R.G., Yarger, F.L., "Shock-Wave Compression of Twenty-Seven Metals," Physics Review 108, No. 2, 196-216.

(20) Huang, Y.K. and Davids, N., "Shock Dynamics of Hypervelocity Impact on Metals," to appear in Journal of Franklin Institute.

(21) Shear, R.E., "Detonation Properties of Pentolite," Ballistics Research Laboratories Report No. 1159.

(22) Rice, M.H., McQueen, R.G., and Walsh, J.M., "Compression of Solids by Strong Shock Waves," Solid State Physics, Advances in Research and Applications, Vol. 6, Academic Press, 1961.

(23) Davids, N., Calvit, H.H. and Johnson, O.T., "Spherical Shock Waves and Cavity Expansion in Metals," Proc. of Sixth Hypervelocity Impact Symposium, Cleveland, Ohio, 1963.

(24) Hill, R., The Mathematical Theory of Plasticity, Oxford Press, 1950.

(25) Stoker, J.J., Nonlinear Vibrations, Interscience Publishers, 1950.